COMMERCIAL

AEEW-R185

A Preliminary Survey of the Void Coefficient of S.G.H.W.

by

D. C. LESLIE

and

P. A. B. MURDOCH*

- SUMMARY -

The void coefficient of S.G.H.W. reactors has been surveyed over a wide range of lattice parameters using the 5-group and 2-group schemes of calculation developed for this type of reactor. The results have been used to infer the dependence of the void coefficient on the lattice parameters, to assist in the specification of the Winfrith experimental programme on S.G.H.W., and to suggest how the design of a power reactor should be modified to achieve an acceptable void coefficient at the start of life.

It is concluded that, according to the 5-group scheme, the void coefficient may be reduced by reducing the pitch, by squeezing water out of the cluster (though if V_{D_2O}/V_{UO_2} is allowed to increase at the same time, most of the effect will be lost), by increasing the enrichment, and by using pins about 0.4" in diameter. The coefficient is insensitive to moderator and coolant temperature, and is increased by any departure from a regular fuel arrangement.

A.E.E.,
Winfrith.

July, 1962

W.5040

---

*Attached from Babcock and Wilcox, Ltd.

CONTENTS

1. Introduction

Two complete computer schemes are at present available for studying the lattice physics of PTHW reactors. These are the Winfrith 5-group scheme (1) and the SGHW series of 2-group programmes (2). Studies reported in reference 3 showed that the two schemes were in flat disagreement over the void coefficient of reactivity of the "old" 61-rod SGHW power reactor: a parameter list for this reactor is given in reference 3. The 2-group scheme suggested that the void coefficient (as defined below) was only just positive, while the 5-group scheme indicated that it was markedly positive.

Calculations using more elaborate and fundamental methods tended to support the verdict of the 5-group scheme that this 61-rod design would have an unacceptably positive void coefficient. To assist in the planning of an experimental programme aimed at elucidating the void coefficient of an SGHW boiling channel, a survey was made, with both schemes, of all the SGHW type cores which could be constructed with the fuel and lattice plates then available at Winfrith.

The reasoning which led to the selection of the experimental programme which is now (June 1962) under way is briefly discussed in section 7 and will be reported in detail elsewhere. When the results of the survey were studied, certain general principles governing the value of the void coefficient began to emerge. The survey was therefore continued in order to clarify these principles, and the present Report is concerned with the findings of this survey. The main emphasis is on the predictions of the 5-group scheme, though there is extensive reference to the 2-group scheme and some comparison with more sophisticated methods of calculation. It must be remembered that the 5-group scheme is not necessarily reliable for the calculation of void coefficients (though present evidence is encouraging) and that the conclusions of this report must be treated with reserve until they have been compared with experiment.

The 5-group calculations have all been made with the Mercury programmes SANDPIPER III (4) and ARISTOS (5). The Fortran programme METHUSELAH (6) became available during the course of this study. Both the physics and the nuclear data of METHUSELAH are slightly different from those of SANDPIPER/ARISTOS, and the void coefficients given by METHUSELAH do not agree exactly with those given by SANDPIPER-ARISTOS; the differences have been carefully reviewed by Allen (7). Although METHUSELAH is presumed to be more accurate than the Mercury programmes, its adoption in this survey would have meant repeating all the work done before it became available.

The discussion in this Report is confined to clean unpoisoned lattices, though some consideration is given to the effects of temperature.

2. Review of general principles

2.1 The definition of void coefficient. We have chosen to define the void coefficient V_c as

$$V_c = 100 \left[k_\infty \ (\rho = 0.4) - k_\infty \ (\rho = 0.8) \right] \% \qquad (2.1)$$

where ρ is the coolant density in gm/cc. k_∞ is evaluated in a reactor which is axially uniform and which has a uniform lattice in the radial direction. Therefore no account is taken in the calculation of either the radial and axial form factors, nor of the variation of coolant density both up the channel and across the fuel cluster. The radial form factor should be adequately accounted for by the usual radial averaging procedures. Moxon (8) has shown that, in one case at least, replacing a flat distribution of bubbles across the fuel cluster by the variation of density suggested by current views on bubble dynamics makes almost no difference to the void coefficient. The effect of the axial variation of neutron flux and coolant density is currently being studied with the programme STAGNANT (9), and this work will be reported in due course.

It will be seen from equation (2.1) that a positive void coefficient implies a gain in reactivity as the coolant density is reduced. Thus a positive coefficient is destabilising whereas a negative coefficient is stabilising. [Fell and co-workers (10) have shown that if V_c is very negative, a different kind of instability may ensue.]. Since leakage always increases as the coolant density ρ is decreased, the void coefficient of k_{eff} is always less than that of k_∞, though the difference is not large for a big power reactor. The present design aim is to ensure that the void coefficient as defined by equation (2.1) is near zero.

In present SGHW designs, saturated water enters the channel at a density of about 0.7 gm/cc. The exit quality is about 13%, corresponding to an exit density of about 0.2 gm/cc., and the channel - averaged density is about 0.4 gm/cc. The reactivity held in voids is therefore approximately

$$\frac{k_\infty \ (\rho = 0.4) - k_\infty \ (\rho = 0.7)}{k_\infty \ (\rho = 0.4)} \qquad (2.2)$$

and V_c somewhat overestimates this quantity. However V_c is more convenient to compute, and serves to reveal general trends just as well as the quantity (2.2). In some cases, the curve of k_∞ against ρ may have "wiggles" in it, and then no one parameter gives a complete guide to stability.

It should be noted that, because of the multiplying factor 100, V_c is a number of the order of unity.

2.2 Qualitative discussion of the effect of changing the coolant density. The void coefficient is, in effect, the first derivative of k_{∞} with respect to the coolant density ρ. The change of V_c with (for example) the size of the fuel pins is a second derivative, and it is to be expected that it will be very difficult to predict. In fact, certain general principles have become clear and these are reviewed below. From the extended discussion given in subsequent sections it will be seen that, while some effects are reasonably clear cut and predictable, others are so complex that trends can only be discovered by computation.

2.2.1 The thermal region. Hydrogen has quite a large thermal absorption (σ_{a0} = 330 mb) and it is to be anticipated that the thermal utilisation f_5 will increase as ρ is reduced, since this reduction removes parasitic absorber from the lattice. Thus a first expectation is that the contribution of the thermal region to V_c will always be positive. However, a reduction in ρ also changes the thermal spectrum in the fuel bundle, the hyperfine structure in the fuel pins and the fine structure across the lattice cell. The absorption rate in the pressure and calandria tubes will therefore change relative to that in the fuel. The sign and magnitude of these subsidiary effects is by no means obvious. They are discussed in Sections 4.5 and 4.6 below, where it is concluded that in SGHW at least they will never outweigh the simple removal of absorber: thus in SGHW the simple expectation is correct.

2.2.2 The resonance region. The resonance escape probability may be written

$$p = \frac{\Sigma_r'}{\Sigma_a' + \Sigma_r'}$$

where Σ_a' and Σ_r' are cell-averaged removal and absorption cross-sections in the resonance region. Since hydrogen is a resonance neutron remover but not an absorber, it might be expected that draining out coolant would reduce p; this implies that the contribution of the resonance region to V_c is negative. However, as in the thermal region, there is a complicating side effect. The SGHW has a cluster-type fuel element, and the coolant acts as a source of resonance neutrons between the pins, as well as a remover. As coolant is drained out, this source is reduced and the amount of resonance absorption will be diminished. (Another way of describing this phenomenon is to say that as the coolant is drained out the mutual shadowing of the fuel pins - the Dancoff-Ginsburg effect - is increased with a consequent reduction in resonance integral. Yet another way of expressing this is to say that interference between the pins reduces their effective surface.). Computations presented later in this report show that at sufficiently low coolant densities the second effect will outweigh the first. However, it does seem that for SGHW reactors the contribution of the resonance region to Vc is negative over the range of coolant density which is of operational interest.

2.2.3 Fast effect. The main effect of collisions with coolant nuclei is to degrade fast neutrons below the fission threshold of U-238. The

opposing tendency, to retain within the fuel cluster neutrons which might otherwise have escaped into the bulk moderator, is small. Thus draining out coolant must increase the fast effect, and the contribution of the fast region to V_0 is always positive.

2.2.4 Presentation of sample numerical results. Results for the old 61-rod power reactor are presented in reference 3. Here we use one of the cores which is being studied in the Winfrith experimental programme as an illustration. This core has:

Fuel: 2.5 Co UO_2, pellet diameter 0.5", canned in 0.036" Al
Fuel geometry: 37 rods in 4 concentric rings
Coolant: H_2O of various densities at room temperature (20°C.)
Pressure tube: Al, inside diameter 4.52", thickness 0.128"
Calandria tube: Al, inside diameter 5.52", thickness 0.192"
Bulk moderator: D_2O of 99.7% purity at room temperature, on an equivalent square pitch of 9.50".

Except for the temperature, this core is quite similar to that of the "new" 37-rod power reactor; a parameter list for this reactor is given in Section 7.

Table I below shows the predictions of the 5-group scheme for this core.

Table I

5-group predictions for the 37/0.5/2.5/452/9.5 core

ρ (gm/cc)	$(\eta f)_t$	p	ε	$(\eta f)_f$	k_∞
0.2	1.5430	0.7632	1.0352	0.6087	1.3218
0.4	1.5168	0.7726	1.0340	0.5831	1.3046
0.6	1.4952	0.7854	1.0336	0.5753	1.2979
0.8	1.4755	0.7972	1.0328	0.5712	1.2922

$V_0 = + 1.21\%$

Here $(\eta f)_t$ and $(\eta f)_f$ are the ratios of the fission yield cross-section ($\nu\Sigma_f$) to the absorption cross-section in the thermal and fast groups (0 to 0.625 e.V. and 0.625 e.V. to 10 Mev respectively) formed by a 2-group condensation of the original 5 groups: this condensation is described in reference 5. p is here defined by

$$\frac{\Sigma_{rf}}{\Sigma_{af} + \Sigma_{rf}}$$

the cross-sections being averaged over the whole of the above-thermal region. k_∞ is then given by

$$k_\infty = (\eta f)_t (1-p) + (\eta f)_f p$$

Finally, $\varepsilon - 1$ is defined as the ratio of the fission yield in the top group of the 5-group scheme (above the fast fission threshold) to the fission yields in the other 4 groups. Table II shows the predictions of the two-group scheme for the same core:

Table II

2-group predictions for the 37/0.5/2.5/452/9.5 core

ρ (gm/cc)	$\eta_5 f_5$	p	ε	k_∞
0.2	1.4820	0.8524	1.0319	1.3036
0.4	1.4686	0.8585	1.0307	1.2994
0.6	1.4567	0.8649	1.0295	1.2970
0.8	1.4457	0.8714	1.0284	1.2956

$V_o = + 0.38\%$

These tables show that, according to both schemes, ηf and ε give positive contributions to V_o, while p gives a negative contribution: this is in agreement with the remarks of the preceding 3 paragraphs. It will also be seen that the 5-group void coefficient is more positive than the 2-group one. This seems to be always so, although the magnitude of the difference varies widely. The results in Tables I and II are shown graphically in figure 1.

In reference 3, an attempt was made to locate the discrepancy between the two schemes by comparing the variations with coolant density of the quantities $\eta f, \varepsilon p$. It was provisionally concluded that the discrepancy was in the thermal region, and that more sophisticated methods of calculation supported the 5-group account of thermal events. Further work by Green (11) suggests that, owing to the very different interpretation put on the symbols ηf, p and ε in the two schemes, this conclusion is not entirely correct: about half the discrepancy is due to the differing treatment of resonance capture. Calculations by Briggs (12) using the Monte Carlo programme MOCUP suggest that although the Hicks correlation (13) (which is used in the 5-group scheme) overestimates p, it reproduces correctly the variation of p with ρ, over the range of interest. This supports the view that the 5-group value of V_o for the old power reactor is nearly correct. A similar study is now being made for the new power reactor.

3. Discussion of some detailed physics effects.

3.0 Arguments concerning the influence of certain detailed physics effects on void coefficient are presented here.

3.1 Thermal spectrum. It would seem at first sight that when coolant is removed from an already undermoderated system, the thermal spectrum in the fuel region must become harder. It is shown in reference 3 that this is not so in the old 61-rod power reactor. In fact, in this reactor the mean value in the fuel of σ_{a5} (W), the Westcott absorption cross-section of U-235, is almost independent of ρ. This quantity is chosen as a criterion of the variation of the thermal spectrum since the thermal utilisation may be written

$$f_5 = \frac{\sigma_{a5}(W)}{\sigma_{a5}(W) + \sigma_c}$$

where σ_c is the number of barns of $\frac{1}{v}$ absorber (duly flux-weighted) per U235 atom.

To discover whether the result referred to above is general, the variation of σ_{a5} (W) with ρ has been computed in a typical experimental core: the results are given in Table III below.

Table III

Variation of $\sigma_{a5}(W)$ with ρ in a 37/0.5/452/9.5" core

ρ (gm/cc)	$\sigma_{a5}(W)$
0.2	651.9 barns
0.4	648.2
0.6	647.0
0.8	646.8
1.0	646.7

It will be seen that once again σ_{a5} (W) is very insensitive to coolant density, and that the mean spectrum in the fuel actually gets very slightly softer as coolant is removed. The change in $\sigma_{a5}(W)$ contributes about + 0.07% to V_c; this is not significant.

3.2 Thermal fine structure. The flux disadvantage factor in the fuel increases almost linearly with κ_u, the inverse diffusion length in the fuel. When coolant is removed both the average absorption and the average transport cross-sections of the fuel region are reduced and therefore κ_u is also reduced. Thus removal of coolant may be expected to reduce the thermal fine structure. This is confirmed by the results given in Table IV for the 37/0.5/2.5/452/9.5 lattice, which we are using as an example throughout this and the previous section.

Table IV

Fine structure factors according to the 5-group scheme for the 37/0.5/2.5/452/9.5 lattice

ρ (gm/cc)	G	GR	GRS
0.2	1.4127	1.5461	2.0041
0.4	1.4852	1.6270	2.0352
0.6	1.5463	1.6980	2.0762
0.8	1.5994	1.7607	2.1179

Here G is the ratio of the mean flux in the pressure tube to the mean flux in the fuel

GR is the ratio of the mean flux in the calandria tube to the mean flux in the fuel

GRS is the ratio of the mean flux in the bulk moderator to the mean flux in the fuel.

(This conforms to the standard notation for physics calculations on graphite reactors.)

This sort of behaviour has been found in all the cores examined so far, and it seems clear that fine structure variations will always make V_c more positive. Part of the discrepancy between the two-and five-group schemes is now known to lie in their accounts of fine structure. Comparison with experiment and with more elaborate calculations suggests that the 5-group scheme is nearer the truth, but it must be remembered that the calculation of fine structure in a cluster fuel element is a particularly difficult matter.

The discussion of hyperfine structure is deferred to sub-section 4.5, where the effect of pin size on V_c is examined. It will be clear that hyperfine structure also decreases as ρ is decreased, and that this further increases the void coefficient.

3.3 The Dancoff-Ginsburg effect. Dresner's first equivalence theorem (14) relates the effective resonance integral of a lumped absorber to that of a homogeneous distribution of the same absorber. It states that the effective resonance integral is a function only of

$$\sigma_p' = \sigma_p + \frac{S}{4NV} \qquad (3.1)$$

where σ_p is the potential scattering per U-238 atom (15.9 barns in UO_2)

N is the number-density of U-238 atoms in the rod

S, V are the surface area and volume of the rod

Rothenstein (15) has shown that in a regular array of rods (3.4) should be generalised to

$$\sigma_p' = \sigma_p + \frac{\gamma S}{4NV} \tag{3.2}$$

where γ is the Dancoff-Ginsburg factor, the reduction in the current of resonance neutrons incident on the surface of the rod due to interception of these neutrons by neighbouring rods. Hicks (13) has used the relation (3.2), and has shown that the functional form

$$RI = -3.43 + 3.10(\sigma_p')^{1/2} \tag{3.3}$$

(both RI and σ_p' being expressed in barns) gives an adequate fit to the best measurements of resonance integral. Hicks uses the Bell approximation to the Dancoff-Ginsburg factor,

$$\gamma = \frac{1}{1 + S/\Sigma_{sm}' V_m} \tag{3.4}$$

where Σ_{sm}' is the macroscopic scattering cross-section of the coolant, and V_m the volume of coolant associated with one fuel pin. (Hicks also has special treatments for the cladding and for the fuel pins on the edge of the cluster, which need not concern us here).

Combining (3.2) and (3.4), we find for circular pins that

$$\sigma_p' = \sigma_p + \frac{\Sigma_{smo}' \rho x}{N_s(1 + 2q.\Sigma_{smo}' \rho x)} \tag{3.5}$$

where q is the pin radius and Σ_{smo}' the macroscopic scattering cross-section of the coolant at unit density, while

$$x = \frac{V_{H_2O}}{V_{UO_2}} \tag{3.6}$$

is the ratio of coolant volume to fuel volume.

Since equation (3.3) implies that the resonance integral increases monotonically with σ_p' the following conclusions can be drawn at once from equation (3.5):

(i) The resonance integral is a monotonically increasing function of coolant density.

(ii) This change in resonance integral is smaller for large pins.

While the above deduction is based on the use of the Hicks correlation, it is likely that the conclusions are generally true.

The resonance integral is not of direct importance. The significant quantity is the resonance escape probability p, which in the 5-group scheme is roughly given by

$$p = \frac{\sigma_{3r}^{*} - 0.46\sigma_{3a}}{\sigma_{3r}^{*} + 0.54\sigma_{3a}} \qquad (3.7)$$

Here σ_{3r}^{*} is the raw group 3 removal cross-section per U-238 atom, given (for an SGHW) by

$$\sigma_{3r}^{*} = 0.836(x\rho + y) \quad \text{(barns)}$$

where

$$y = \frac{V_{D_2O}}{V_{UO_2}} \qquad (3.8)$$

is the ratio of bulk moderator volume to fuel volume. Also, σ_{3a}, the group 3 absorption cross-section, is given by

$$\sigma_{3a} = -0.436 + 0.341(\sigma_p')^{1/2} \quad \text{(barns)}$$

The above formulae oversimplify the physical situation, since they ignore removals in the cladding, PT and CT, any fine structure in the group 3 flux, and captures by U-235 in group 3. The first two effects are not very important, but in a typical SGHW about 25% of all group 3 captures occur in U-235. In ignoring these captures we overestimate p, but do not seriously alter the variation of p with ρ and g.

Figure 2 shows the variation of p with ρ for a reactor with x= 1.2 and y = 6 (these values being quite close to those for the current 37 rod power reactor), and with both 0.3" and 0.5" pins. A positive slope on this graph implies a negative contribution of p to V_0. Therefore the figure shows that the contribution of p to V_c is negative over the operating range of densities, but becomes positive for very low densities. It should be re-iterated that figure 1 is based on the Hicks correlation (13). Calculations with the Monte Carlo programme MOCUP confirm the trend of p with ρ for ρ greater than 0.3 gm/cc. They do not confirm the existence of the dip in the curve at ρ values of about 0.2 gm/cc, though a small dip might be concealed by the statistical fluctuations inherent in the Monte Carlo method.

Figure 1 also shows that the negative contribution of p to V_0 in the operating range of densities is larger for the 0.5" pins than for the 0.3" pins. This point will be taken up again in sub-section 4.5, in which the dependence of V_0 on pin size is discussed.

4. Parametric dependence of the void coefficient

In order to achieve the design aim of a near zero V_c, it is necessary to know how V_c varies with the main design parameters of the core (though there are naturally many other constraints on these parameters). The relevant parameters are:-

Size, number and spacing of the fuel pins

Can thickness

Fuel enrichment

Lattice pitch

Diameter and thickness of pressure tubes and calandria tubes

We find it convenient to combine some of these quantities, and to take as our basic parameters the quantities

$$x = \frac{V_{H_2O}}{V_{UO_2}} \quad \text{and} \quad y = \frac{V_{D_2O}}{V_{UO_2}}$$

Sub-sections 4.1 and 4.2 are devoted to a description of the effect on V_c of variations in y and x: these variations are summarised in figures 14 to 23. In 4.3, we show that moderator and coolant temperature have only a minor influence on V_c, while the effect of varying the enrichment and the pin size are discussed in sub-sections 4.4 and 4.5. The effect of pin arrangement and of pressure and calandria tube thickness are investigated in sub-sections 4.6 and 4.7, and the results are summarised in sub-section 4.8.

The present section is the heart of this report. Previous sections have been descriptive, but we now present the large number of calculations of void coefficient which we have made.

4.1. The effect of varying $y = V_{D_2O}/V_{UO_2}$. Figure 3 shows the variation of V_c with y for the 37/0.5/2.5/452 cores, which we continue to use as an illustration, for both the 5 - and 2 - group schemes. This figure brings out two rules which have been found to be quite general:

(i) V_c is a rapidly increasing function of y over the range of design interest.

(ii) The 5-group value of V_c is larger than the two-group value.

The first rule is of extreme importance to the designer, since change of pitch is the only parameter variation which has a really dramatic effect on V_c. It can be explained quite simply in physical terms. Because of the low thermal absorption of the D_2O bulk moderator, an increase of pitch has little effect on the fast and thermal processes but it increases p by increasing the removal cross-section for resonance neutrons.

It will be recalled that the contribution of resonance capture to V_c is negative; as the amount of resonance capture decreases, this contribution will diminish, and V_c will therefore increase.

This argument can be put into mathematical form. Table V shows that the variation of $(\eta f)_t$ and $(\eta f)_f$ with pitch is very much less strong than that of p.

TABLE V

Breakdown of k_∞ for a 37/0.5/2.5/452 core at square pitches of 8.84", 9.5" and 11.02", according to the 5-group scheme.

Pitch	y	ρ	$(\eta f)_t$	$(\eta f)_f$	þ
8.84"	7.243	0.4	1.5198	0.5732	0.7417
		0.8	1.4798	0.5634	0.7746
9.5"	8.970	0.4	1.5168	0.5830	0.7726
		0.8	1.4754	0.5712	0.7972
11.02"	13.408	0.4	1.5109	0.6045	0.8199
		0.8	1.4670	0.5897	0.8332

It is shown in the Appendix that if the variation of $(\eta f)_t$ and $(\eta f)_f$ with pitch is ignored, then

$$\frac{\partial V_c}{\partial y} = 100\left[(\eta f)_t - (\eta f)_f\right] \frac{0.836\,\sigma_{3a}}{\{0.836(x\rho + y) + 0.54\sigma_{3a}\}^2}\Bigg|_{\rho=0.8}^{\rho=0.4} \qquad (4.1)$$

This equation shows that if $(\eta f)_t$ and $(\eta f)_f$ were truly independent of pitch, then $\partial V_c/\partial y$ would always be positive and that it would diminish as y was increased: more detailed investigation shows that the variation of the ηf-s with pitch is not large enough to invalidate these conclusions. This flattening-off of the variation of V_c with y indicated by this equation is illustrated in figures 14 to 23, which show that these rules apply to both schemes of calculation and to all cores.

It also appears that the difference in void coefficient between the two schemes is insensitive to V_{D_2O}/V_{UO_2} ratio. This may be seen (for example) in the old 61 rod power reactor at room temperature, results for which are given in Table VI:

TABLE VI

Void coefficient of the old 61 rod power reactor at various pitches, according to both schemes.

61/0.43/546/2Co				
Pitch	y	V_c (5gp)%	V_c (2gp)%	Difference
8.5"	3.70	-2.22	-4.53	2.31
9.5"	5.74	0.64	-1.62	2.26
10.5"	7.99	2.53	0.32	2.21
11.5"	10.48	3.79	1.66	2.13

Similar results have been found in all other cases studied.

4.2. Variation of void coefficient with $x = V_{H_2O}/V_{UO_2}$. In all cases so far considered it has been found that the void coefficient increases with $x = V_{H_2O}/V_{UO_2}$. This can be clearly seen from the contour maps given in Figures 24 to 28; the contours are of constant void coefficient in the x, y plane.

Table VII below shows the variation of V_c with x for a 37-rod cluster of 0.5" 2.5 Co rods in various pressure tubes and at various pitches.

TABLE VII

x	Pressure Tube	37/0.5/2.5Co: 5-group					
		Pitch					
		8.84"		9.5"		11.02"	
		V_c %	y	V_c %	y	V_c %	y
0.844	452	0.21	7.24	1.24	8.97	2.69	13.41
1.390	503	0.43	6.56	1.76	8.29	3.73	12.73
1.635	525	0.60	6.23	2.01	7.96	4.16	12.39

These results are plotted in figure 4. From this figure it will be seen that V_c increases with x, and that $\partial V_c/\partial x$ is an increasing function of pitch. However, the curves on figure 4 are contours of V_c against x at constant pitch, while the analysis of sub-section 3.3 shows that the fundamental parameter is y rather than the lattice pitch. Now if the pressure and calandria tube radii are increased while the lattice pitch is held constant, y must be reduced: this trend is clearly shown in Table VII. Since $\partial V_c/\partial y$ is positive (this was established in the previous sub-section), this reduction in y will cause a decrease in V_c which tends to mask the increase due to increasing x. Figure 5 therefore presents the void coefficient at constant y rather than at constant pitch (this is done by graphical interpolation from figure 4 which, although rather inaccurate, suffices to show the trends). It will be seen that $\partial V_c/\partial x$ is now markedly positive for all values of y. The difference between figure 4 and figure 5 can be explained by observing that a given change in calandria tube radius makes a bigger proportional change in y when the pitch is small than when it is big. Figure 6 shows similar behaviour for a 37-rod cluster of 0.5" rods enriched to 1.28 Co, confirming that the trends of figures 4 and 5 are general.

This trend can also be understood theoretically. It is shown in the Appendix that if the consequences of fine structure and the Dancoff-Ginsburg effect are ignored, then

$$\frac{\partial V_c}{\partial x} = 100\left[\{(\eta f)_t - (\eta f)_f\}\frac{0{\cdot}836\,\sigma_{3a}\rho}{\{0{\cdot}836(x\rho+y)+0{\cdot}54\,\sigma_{3a}\}^2} - \alpha\eta b\rho f^2\right]_{\rho=0{\cdot}8}^{\rho=0{\cdot}4} \qquad (4.2)$$

α being a positive constant. The first term of this equation is similar to the right-hand side of equation (4.1); the contribution of this first term is therefore positive, while the second is obviously positive (since the constant $\alpha > 0$). Thus, provided fine structure and the Dancoff-Ginsburg effect can be ignored, $\partial V_c/\partial x$ is positive. Only computation can show that these effects do not reverse the simple conclusion: this indicates why it has been necessary to use computer programmes rather than simple analysis for the present investigation.

4.3. Coolant and moderator temperature. It is not to be expected that the void coefficient will depend strongly on these temperatures: the applicability of the results of this Report to the start-of-life conditions in power reactors rests on this assumption. All the results quoted with the exception of those in this section are calculated with both the coolant and bulk moderator at room temperature, and it is assumed that relevant deductions can then be drawn for the corresponding power reactor at hot working conditions. The results presented below show that in one case at least this assumption is well-founded. These results have already been presented in reference 3 but it seems worth-while re-presenting them here for the sake of completeness.

Computations have been carried out, using both the 5 - and 2 - group schemes, on the old 61 rod power reactor at four coolant temperatures ranging from room temperature to operating conditions, and the results are shown in Table VIII and Figure 7.

TABLE VIII

Dependence of void coefficient on coolant and moderator temperatures, according to both schemes

$T(^{\circ}C)$ coolant	$T(^{\circ}C)$ moderator	5 gp. V_c (%)				2 gp. V_c (%)			
Pitch		$8\frac{1}{2}$"	$9\frac{1}{2}$"	$10\frac{1}{2}$"	$11\frac{1}{2}$"	$8\frac{1}{2}$"	$9\frac{1}{2}$"	$10\frac{1}{2}$"	$11\frac{1}{2}$"
20	20	-2.22	0.64	2.53	3.79	-4.53	-1.62	0.32	1.66
100	38.7	--	0.82	2.70	3.95	--	-1.73	0.24	1.59
180	57.4	--	0.90	2.75	4.00	--	-1.82	0.18	1.55
277	80	-1.74	1.07	2.91	4.14	-5.03	-1.92	0.13	1.52

It is apparent that the void coefficient is comparatively insensitive to coolant and moderator temperatures in the old (61 rod) power reactor. The small variation which does exist is in the opposite direction for the 5-group and 2-group schemes; the void coefficient for a pitch of about 10" increases slightly with rising temperature according to the 5-group scheme, and falls according to the 2-group scheme.

It should be mentioned that no allowance is made for the Doppler coefficient of the resonance integral in the SANDPIPER - ARISTOS calculations (although such an allowance is made in METHUSELAH): a cold resonance integral is used throughout. It is plausible on physical grounds that the effect of this omission on V_c will be negligible, though it will alter the "level" of k_∞.

4.4. The effect of enrichment. It is fairly obvious that increasing the enrichment will reduce the void coefficient, since as the U-235 content of the fuel grows, the competition of the hydrogen in the coolant for thermal neutrons becomes less important. This argument can be put on a formal basis. Since f_t is the only parameter which is seriously affected by changing the enrichment, we have

$$\frac{\partial V_c}{\partial C_o} = \eta_t \phi \left.\frac{\partial f_t}{\partial C_o}\right|_{\rho=0.8}^{\rho=0.4} = -\eta_t \phi \int_{0.4}^{0.8} \frac{\partial^2 f_t}{\partial \rho \partial C_o} d\rho \qquad (4.3)$$

This quantity may be symbolically expressed as

$$f_t = \frac{C_o}{C_o + a + b\rho + eG} \qquad (4.4)$$

where a, b and e are constants. The last term in the denominator represents the effect of fine and hyperfine structure. If we ignore the variation of fine structure with C_o and ρ, we find

$$\frac{\partial^2 f_t}{\partial \rho \partial C_o} = \frac{b(C_o - a - b\rho - eG)}{(C_o + a + b\rho + eG)^3} = b\left(\frac{C_o}{f_t}\right)^2 (2f_t - 1)$$

Therefore, from (4.3) and (4.4), $\partial V_c / \partial C_o$ is certainly negative if $f_t > \frac{1}{2}$, a condition which is comfortably met in all the lattices considered so far. The effect of fine structure is complex: it increases with both ρ and C_o, and these influences act in opposite directions. However, the computations reported below show that the simple theory does give the correct conclusion.

Various results are available to display this change of void coefficient with enrichment and those for the 37/0.5/503 lattice are shown in Table IX and Figure 8.

TABLE IX

Change of void coefficient with enrichment for 37/0.5/503 clusters

5 group

Co	Pitch 8.84" y = 6.56	Pitch 9.5" y = 8.29	Pitch 11.02" y = 12.73
1.28	2.04	3.14	4.77
2.0	1.08	2.34	4.20
2.5	0.43	1.76	3.73
2 group			
1.28	0.93	2.00	3.59
2.0	-0.45	0.82	2.71
2.5	-1.20	0.16	2.18

The clusters 37/0.5/452, 90/0.3/525, 37/0.5/525 have also been studied at various enrichments. Results for these calculations are given in Table X and are

plotted in Figures 9, 10, 11.

TABLE X

General comparison of 5-group and 2-group predictions of V_o

	Pitch / C_o	8.84"	9.5"	11.02"	
37/0.5/452	1.28	1.33	2.21	3.39	5 gp.
	2.0	0.72	1.70	3.07	
	2.5	0.21	1.24	2.69	
	1.28	0.51	1.35	2.49	2 gp.
	2.0	-0.19	0.89	2.43	
	2.5	-0.65	0.38	1.80	
90/0.3/525	1.6	1.65	2.80	4.46	5 gp.
	2.0	1.12	2.46	4.30	
	2.5	0.40	1.71	3.66	
	1.6	1.35	2.49	4.22	2 gp.
	2.0	0.65	1.95	3.80	
	2.5	-0.43	0.89	2.92	
37/0.5/525	1.28	2.50	3.67	5.47	5 gp.
	2.0	1.22	2.50	4.53	
	2.5	0.60	2.01	4.16	
	1.28	1.82	2.91	4.59	2 gp.
	2.0	0.15	1.45	3.45	
	2.5	-0.78	0.60	2.83	

It will be seen that the two-group scheme also predicts a reduction of void coefficient with increasing enrichment. The difference between the predictions of the two schemes increases with increasing enrichment; this is believed to be due to the differing treatment of fine structure in the two methods of calculation.

A breakdown of the results of a 5-group analysis is given in Table XI, for

a 37/0.5/503 lattice with 9.5" square pitch, whence it can be seen that the dependence of resonance escape on enrichment is very much smaller than the dependence of thermal utilisation, which, as expected, increases strongly with increasing enrichment.

TABLE XI

Dependence of the components of k_∞ on enrichment for a 37/0.5/503 cluster at 9.5" pitch, according to the 5-group scheme

Co	$(\eta f)_t$		$(\eta f)_f$		p	
	$\rho = 0.4$	$\rho = 0.8$	$\rho = 0.4$	$\rho = 0.8$	$\rho = 0.4$	$\rho = 0.8$
1.28	1.1939	1.1246	0.4124	0.4146	0.7971	0.8301
2.0	1.3881	1.3227	0.5016	0.4974	0.7861	0.8214
2.5	1.4831	1.4214	0.5575	0.5498	0.7778	0.8149

4.5. The effect of pin size. The investigation of this effect is the most complex of all the studies in this survey. A comparison of the contour maps for the 2.5 Co 0.3" and 2.5 Co 0.5" lattices given in figures 27 and 28 shows that increasing the pin size from 0.3" to 0.5" increases the void coefficient (though it must be remembered that these graphs are drawn on the assumption that the detailed arrangement of the pins is not important). In order to check this conclusion, a special investigation has been made on three lattices, namely

37/0.5/525/2.0
61/0.3827/525/2.0
91/0.3133/525/2.0

in which all parameters have been held constant with the exception of the number of pins and the pin radius: this large pressure tube has been selected because it gives some flexibility in the arrangement of the cluster. The number of pins and the pin radius have been varied in such a way that the fuel volume is the same in all 3 lattices, and the pins are arrayed regularly. Thus x and y, and also the volumes of the cans, the pressure tube and the calandria tube are the same in all cases.

These results which are presented in detail later in this sub-section, show that the void coefficient first decreases and then increases with increasing pin-size. This is due to the effect on the void coefficient of the detailed disposition of the fuel rods. It is to be expected that the net effect on Vc of variation of pin size will depend on the interplay of two opposing consequent effects, namely

the variations in resonance escape and in hyperfine structure. The resonance escape probability is found to increase with increasing pin radius, and the hyperfine structure in each pin cell also becomes more pronounced as the pin radius is increased. The latter effect leads to a lower mean flux in the fuel pins and a consequent decrease in the thermal utilisation. For the results currently available however, it has been found that the effect of pin size on void coefficient is partially obscured by variations in thermal fine structure caused by differing fuel dispositions.

The effect of pin size on p is discussed in sub-section 3.3. From the computations reported there it follows that the contribution of p to V_c, which may be defined as

$$100 \left[p(0.4) - p(0.8) \right]$$

is -2.74 for 0.3" pins and -3.10 for 0.5" pins, with x = 1.2 and y = 6. The increase of pin size therefore reduces the contribution of p to V_c by 0.36: the reduction for x = 1.2 and y = 8 is 0.35, which is almost the same. Since V_c is actually found to increase when the pin diameter is increased from 0.3" to 0.5", there must be an effect in the thermal region which overrides this reduction due to the resonance region. This is clearly shown by Tables XII, XIII and XIV below.

Table XII gives k_∞ at ρ = 0.4 and ρ = 0.8 for the three cores studied, namely 37/0.5/525/2.0 Co, 61/0.3827/525/2.0 Co, and 91/0.3133/525/2.0 Co, at the three standard pitches, 8.84" square, 9.5" square and 11.02" square. The table also gives the void coefficients, which are also plotted in figure 12.

TABLE XII

Variation of k_∞ with pitch and pin size for 3 clusters with the same pin size, according to the 5-group scheme

Cluster \ Pitch	8.84"		9.5"		11.02"	
	ρ = 0.4	ρ = 0.8	ρ = 0.4	ρ = 0.8	ρ = 0.4	ρ = 0.8
37/0.5/525/2.0	1.1765	1.1623	1.1991	1.1716	1.2338	1.1863
V_c =	1.42		2.75		4.75	
61/0.3827/525/2.0	1.1753	1.1689	1.2002	1.1809	1.2388	1.2004
V_c =	0.64		1.93		3.84	
91/0.3133/525/2.0	1.1682	1.1607	1.1936	1.1728	1.2331	1.1926
V_c =	0.75		2.08		4.05	

It will be seen that at all 3 pitches, V_c has a minimum for pins of about 0.4" diameter. In order to discover whether this behaviour was affected by enrichment (as might well be the case, since it is partly due to hyperfine structure) the computations were repeated for the same 3 clusters, namely 37/0.5/525, 61/0.3827/525 and 91/0.3133/525, at an enrichment of 2.5 Co. The results of this second set of computations are also shown on figure 12. It will be seen that once again V_c is a minimum for 0.4" pins, and that the increased enrichment has reduced the void coefficient: this is in agreement with the findings of the previous sub-section.

Tables XIII and XIV give values of p, $(\eta f)_t$ and $(\eta f)_f$ for these same cases, and also list the differences in these quantities as ρ is increased from 0.4 to 0.8

TABLE XIII

Variation of p with pitch and pin size for 3 clusters with the same fuel volume, according to the 5-group scheme

Pitch / Cluster	8.84"		9.5"		11.02"	
	ρ = 0.4	ρ= 0.8	ρ= 0.4	ρ= 0.8	ρ= 0.4	ρ= 0.8
37/0.5/525/2.0	0.7650	0.8154	0.7922	0.8316	0.8356	0.8592
Δp =	- .0504		- .0394		- .0236	
61/0.3827/525/2.0	0.7574	0.8073	0.7856	0.8245	0.8308	0.8539
Δp =	- .0499		- .0389		- .0231	
91/0.3133/525/2.0	0.7534	0.8024	0.7821	0.8201	0.8281	0.8501
Δp =	- .0490		- .0380		- .0220	

From Table XIII, it will be seen that the contribution of p to the void coefficient is reduced (or rather, the negative contribution is increased) by increasing the pin size. This reduction is rather less than that derived from the computations leading to figure 1. This is because the quantity calculated in figure 1 is not quite the same as that listed in Table XIII (the quantity in Table XIII is the probability of escape from the fast group, and therefore includes fast capture in U-235 and fast fission). A correction is also required for the fact that figure 1 is for an infinite cluster, while Table XIII is for finite clusters.

Table XIV shows the results for $(\eta f)_t$ and $(\eta f)_f$: the anomalous variation of $(\eta f)_t$ with pin size is clearly apparent.

TABLE XIV

Variation of $(\eta f)_t$ and $(\eta f)_f$ with pitch and pin size for 3 clusters with the same fuel volume, according to the 5-group scheme

$(\eta f)_t$

Cluster \ Pitch	8.84"		9.5"		11.02"	
	$\rho = 0.4$	$\rho = 0.8$	$\rho = 0.4$	$\rho = 0.8$	$\rho = 0.4$	$\rho = 0.8$
37/0.5/525/2.0	1.3854	1.3129	1.3813	1.3071	1.3729	1.2956
$\Delta(\eta f)_t =$	+ .0725		+ .0742		+ .0773	
61/0.3827/525/2.0	1.3990	1.3351	1.3953	1.3305	1.3877	1.3212
$\Delta(\eta f)_t =$	+ .0639		+ .0648		+ .0665	
91/0.3133/525/2.0	1.3970	1.3330	1.3932	1.3279	1.3855	1.3178
$\Delta(\eta f)_t =$	+ .0640		+ .0653		+ .0677	

$(\eta f)_f$

Cluster \ Pitch	8.84"		9.5"		11.02"	
	$\rho = 0.4$	$\rho = 0.8$	$\rho = 0.4$	$\rho = 0.8$	$\rho = 0.4$	$\rho = 0.8$
37/0.5/525/2.0	0.4961	0.4976	0.5042	0.5028	0.5271	0.5200
$\Delta(\eta f)_f =$	- .0015		+ .0014		+ .0071	
61/0.3827/525/2.0	0.4773	0.4731	0.4853	0.4779	0.5074	0.4951
$\Delta(\eta f)_f =$	+ .0042		+ .0074		+ .0123	
91/0.3133/525/2.0	0.4687	0.4608	0.4770	0.4660	0.4995	0.4829
$\Delta(\eta f)_f =$	+ .0079		+ .0110		+ .0166	

(It will also be seen that the effect of $(\eta f)_f$ is to make V_c increase with pin size. An inspection of Tables XIII and XIV will convince the reader that the variation of V_c with pin size is beyond the reach of simple calculation). The only effect in the thermal region which is obviously dependent on pin size is the hyperfine structure. It was remarked at the end of sub-section 3.2 that the effect of hyperfine structure is to increase the void coefficient.

Since hyperfine structure increases with pin size, the contribution of $(\eta f)_t$ to V_c might be expected to increase steadily with pin size. Table XIV shows that this is not so.

In order to confirm that the results presented in Table XII are not anomalous, the calculations have been repeated for the same fuel geometry, but at an enrichment of 2.5 Co. These calculations are presented in Table XV below, and in figure 12.

TABLE XV

Variation of k_∞ with pitch and pin size for three clusters of 2.5 Co fuel with the same fuel volume, according to the 5-group scheme

Pitch / Cluster	8.84"		9.5"		11.02"	
	$\rho = 0.4$	$\rho = 0.8$	$\rho = 0.4$	$\rho = 0.8$	$\rho = 0.4$	$\rho = 0.8$
37/0.5/525/2.5	1.2501	1.2441	1.2744	1.2543	1.3122	1.2706
V_c =	0.60		2.01		4.16	
61/0.3827/525/2.5	1.2536	1.2549	1.2807	1.2682	1.3228	1.2899
V_c =	-0.13		1.25		3.29	
91/0.3133/525/2.5	1.2462	1.2452	1.2738	1.2596	1.3167	1.2817
V_c =	0.10		1.42		3.50	

It will be seen that the void coefficients for 2.5 Co fuel show exactly the same trend with pin size as those for 2.0 Co fuel. It is now clear that the behaviour suggested by Table XII is not an isolated anomaly, but a phenomenon requiring further study.

An obvious complication is the effect of fine structure across the cell as opposed to hyperfine structure across the pins. Since the effective fuel cross-section must decrease as the hyperfine structure factor is increased, we would further expect the fine structure factor GRS to decrease as the pin size is increased. Table XVI shows that this expectation is also wrong: it is flatly contradicted by the results for 0.5" pins.

TABLE XVI

GRS for three clusters with the same fuel volume, according to the 5-group scheme: $\rho = 0.4$

Cluster		GRS
37/0.5/525/2.0/9.5"	...	1.7186
61/0.3827/525/2.0/9.5"	...	1.6767
91/0.3133/525/2.0/9.5"	...	1.6990

Calculations have therefore been made with the hyperfine structure removed. This was done by switching out the RIPPLE hyperfine structure subroutine in the SANDPIPER III programme. (The necessary modification to the SANDPIPER programme was made by M. J. Terry). The results of calculations on the 37 and 61 rod clusters are shown in Table XVII.

TABLE XVII

The effect of hyperfine structure on k_∞ for two clusters with the same fuel volume, according to the 5-group scheme

Cluster	V_o (RIPPLE In)	V_o (RIPPLE Out)
37/0.5/525/2/9.5"	2.75	1.70
61/0.3827/525/2/9.5"	1.93	1.12
37/0.5/525/2/9.5	$\rho = 0.4$	$\rho = 0.8$
RIPPLE In } $(\eta f)_t$	1.3813	1.3071
RIPPLE Out }	1.3943	1.3321
61/0.3827/525/2/9.5	$\rho = 0.4$	$\rho = 0.8$
RIPPLE In } $(\eta f)_t$	1.3938	1.3291
RIPPLE Out }	1.4046	1.3486

As expected, removing the hyperfine structure increases $(\eta f)_t$ and reduces both V_o and the change of V_c with pin size. Vc still increases as the pin diameter is increased from 0.3" to 0.5", in spite of the negative contribution of the resonance region, and it is clear that yet another effect is at work. This is confirmed by the comparison of GRS with and without hyperfine structure given in Table XVIII (for $\rho \approx 0.4$).

TABLE XVIII

Comparison of GRS with and without hyperfine structure for two clusters with the same fuel volume, according to the 5-group scheme

CLUSTER	GRS RIPPLE IN	GRS RIPPLE OUT
37/0.5/525/2.0/9.5	1.7186 ...	1.7456
61/0.3827/525/2.0/9.5	1.6767 ...	1.6977

The simple expectation is that, with RIPPLE switched out, GRS should be independent of pin size. This simple expectation is based on the assumption that the detailed disposition of the pins is not important. Table XVIII suggests that this assumption must be wrong, and a limited survey has therefore been made of the effect of pin position.

4.6. The effect of pin position. This has been studied in a 37/0.5/525/2.0 Co lattice at three pitches. In the normal lattice of this kind, the pins are regularly arrayed. Two further cores of this kind have been studied, in which the pins are first packed as closely as possible round the central pin ("Close-packed" cluster) and a second in which all except the central fuel pin are pushed as near to the pressure tube as possible ("Edge-packed" cluster). These three types of fuel arrangement are compared in Figure 13, and their void coefficients are compared in Table XIX.

TABLE XIX

Comparison of V_o for 3 different arrangements of fuel, according to the 5-group scheme

Fuel arrangement \ Pitch	8.84"	9.5"	11.02"
Close-packed	4.18	5.50	7.53
Normal	1.42	2.75	4.75
Edge-packed	2.44	3.24	4.30

It will be seen that close-packing produces a rather disastrous increase in void coefficient, and that the regular arrangement is to be preferred except at large lattice pitches.

It is found that k_∞ is strongly affected by fuel position, being as much as 8% lower in the close-packed arrangement than in the normal one. The breakdown of this variation given in Table XX is very instructive.

TABLE XX

Variation of p and $(\eta f)_t$ with fuel arrangement, according to the 5-group scheme

Fuel arrangement	p		$(\eta f)_t$	
	$\rho = 0.4$	$\rho = 0.8$	$\rho = 0.4$	$\rho = 0.8$
Close-packed	.8030	.8413	1.3490	1.2464
Diff =	- .0383		+ .1026	
Normal	.7922	.8316	1.3813	1.3071
Diff =	- .0394		+ .0742	
Edge-packed	.7950	.8348	1.4189	1.3366
Diff =	- .0398		+ .0823	

p is lower in the normal arrangement than in either of the packed ones, since in the normal arrangement the pin spacing is wider and the Dancoff correction less. The contribution of p to the void coefficient is not much affected by fuel arrangement. $(\eta f)_t$ increases very strongly as fuel is moved from the centre of the coolant channel to its edge: the contribution of thermal effects to V_c is minimised by a regular arrangement of the pins.

These results are also a warning against over-literal use of the contour maps of Figures 24 to 28 (described in section 4.8 below): it is clear that these maps are only valid for regular fuel arrays. It should also be mentioned that the effects discussed in this section are difficult to calculate, and it should not necessarily be assumed that the 5-group scheme is predicting them correctly.

4.7. The effect of pressure and calandria tube thickness. The positive contribution of $(\eta f)_t$ to V_c is due to competition between U-235 and H for thermal neutrons. The introduction of parasitic absorbers must reduce this contribution by reducing the competing effect of the H. (This argument can be formalised after the manner of sub-section 4.2).

An analysis has been carried out on a 37/0.5/2/525 system at various pitches and with two calandria tube thicknesses. The calandria tube was thickened into the air gap rather than the moderator, thus maintaining the value of y. The results of this analysis are given in Table XXI. The conclusion above is borne out, namely that the void coefficient decreases with an increase in calandria tube thickness.

TABLE XXI

Dependence of V_o on pitch for a 37/0.5/2.0/525 core with two different calandria thicknesses, according to the 5-group scheme

	8.84"	9.5"	11.02"
V_o (1)	1.22	2.50	4.53
V_o (2)	1.42	2.75	4.75

V_o (1) is the void coefficient value with the thick calandria tube, V_o (2) that with the thin (standard) one, both calandrias being made of aluminium.

C.T. thickness (1) = 0.319".

C.T. thickness (2) = 0.192"

Although V_o does decrease as the calandria tube is made thicker, the change is too small for there to be any incentive to use a calandria (and pressure) tube any thicker than is demanded by engineering considerations.

These results have been further analysed to show the variation of $(\eta f)_t$, $(\eta f)_f$ and p for the two cores; these values are displayed in Table XXII. It can be seen that, as is expected, increasing the thickness of the calandria tube reduces $(\eta f)_t$ substantially with little effect on the other components of k_∞.

TABLE XXII

Breakdown of k_∞ for a 37/0.5/2.0/525 core with two different calandria thicknesses according to the 5-group scheme

	Pitch	p	$(\eta f)_t$	$(\eta f)_f$	b
THICK (1)	8.84"	0.8	1.2818	0.4925	0.8136
		0.4	1.3509	0.4907	0.7628
	9.5"	0.8	1.2747	0.4890	0.8270
		0.4	1.3458	0.4905	0.7869
	11.02"	0.8	1.2611	0.5037	0.8544
		0.4	1.3362	0.5104	0.8301
THIN (2)	8.84"	0.8	1.3129	0.4976	0.8154
		0.4	1.3854	0.4961	0.7650
	9.5"	0.8	1.3071	0.5028	0.8316
		0.4	1.3813	0.5042	0.7922
	11.02"	0.8	1.2956	0.5200	0.8592
		0.4	1.3729	0.5271	0.8356

The effect of thickening the pressure tube has not been studied in detail, but there is every reason to expect that it will be similar to that of thickening the calandria tube.

4.8. Graphical representation of void coefficient variation. In the previous sections it has been shown that the void coefficient of reactivity increases with both $y = V_{D_2O}/V_{UO_2}$ and $x = V_{H_2O}/V_{UO_2}$, and that it decreases with enrichment. Several other effects have also been discussed. It would be useful if all these effects could be simultaneously displayed, and the general behaviour of the void coefficient made evident. The sets of results and graphs given below is an attempt to achieve this. Figures 14 to 23 are a graphical display of all the results quoted in Tables XXIII to XXVII (which are brought together at the end of this sub-section). These figures are plots of the void coefficient

against y for several x values, at fixed enrichment and pin size according to the 5-group scheme (figures 14 to 18) and the 2-group scheme (figures 19 to 23). The enrichments and pin sizes so far studied in sufficient detail to permit the construction of such tables and graphs are 1.28 Co 0.5", 1.6 Co 0.3", 2 Co 0.5", 2.5 Co 0.3", 2.5 Co 0.5".

The subsequent five figures, (figures 24 to 28) are constructed from these to give contours of constant void coefficient. For example, the 1% void coefficient line according to the 5-group scheme for the 1.28 Co 0.5" cores shown in figure 24 is constructed by plotting the values of x and y at which the three curves in figure 14 intersect the 1% void coefficient line. In this way the expected value of void coefficient for any of the experimental assemblies in the standard pressure and calandria tubes can be read off at a glance. (The fuels listed at the end of the previous paragraph are the four main types of enriched oxide which are currently - June 1962 - held in store at Winfrith together with an additional "imaginary" fuel, namely 2.0 Co 0.5", which was included to clarify the effect of enrichment).

The information which has been detailed in the previous sections is all contained in these contour maps of figures 24 to 28. For example it is immediately evident that the void coefficient increases with increasing $y = V_{D_2O}/V_{H_2O}$ ratio, and that this increase is marked. It is also apparent that the void coefficient in all cases shows an increase with increasing $x = V_{H_2O}/V_{UO_2}$. The decrease of void coefficient with increasing enrichment can be seen by comparing figures 24 and 28 for the 1.28 Co 0.5" and 2.5 Co 0.5" fuels. This decrease is very pronounced. An increase in enrichment of this magnitude can be seen to cause almost 2% reduction in V_c.

It is evident from all these figures that the 5-group scheme always gives a more positive void coefficient than the 2-group scheme, and that the differences between the predictions of the two schemes is very variable. A comparison of figures 24 and 28 shows that the difference between the two schemes increases with enrichment, while figures 27 and 28 show that this difference also increases with pin size.

/Table XXIII .....

TABLE XXIII

1.28 Co 0.5"

	Equivalent square pitch →	8.84"		9.5"		11.02"	
	Cluster type ↓	V_c	y	V_c	y	V_c	y
5 group	37/0.5/525 (x = 1.635)	2.50	6.227	3.67	7.955	5.47	12.392
	37/0.5/503 (x = 1.390)	2.04	6.562	3.14	8.290	4.77	12.727
	37/0.5/452 (x = 0.844)	1.33	7.243	2.21	8.970	3.39	13.408
2 group	37/0.5/525 (x = 1.635)	1.82	6.227	2.91	7.955	4.59	12.392
	37/0.5/503 (x = 1.390)	0.93	6.562	2.00	8.290	3.59	12.727
	37/0.5/452 (x = 0.844)	0.51	7.243	1.35	8.970	2.49	13.408

TABLE XXIV

1.6 Co 0.3"

	Equivalent square pitch →	8.84"		9.5"		11.02"	
	Cluster type ↓	V_c	y	V_c	y	V_c	y
5 group	90/0.3/580 (x = 2.552)	2.94	5.833	4.17	7.751	6.08	12.678
	90/0.3/525 (x = 1.789)	1.65	6.914	2.80	8.832	4.46	13.759
	90/0.3/485 (x = 1.30)	1.32	7.607	2.30	9.525	3.67	14.452
2 group	90/0.3/580 (x = 2.552)	2.73	5.833	3.88	7.751	5.85	12.678
	90/0.3/525 (x = 1.789)	1.35	6.914	2.49	8.832	4.22	13.759
	90/0.3/485 (x = 1.30)	0.83	7.607	1.88	9.525	3.41	14.452

TABLE XXV

2 Co 0.5"

	Equivalent square pitch →	8.84"		9.5"		11.02"	
	Cluster type ↓	V_c	y	V_c	y	V_c	y
5 group	37/0.5/525 (x = 1.635)	1.22	6.227	2.50	7.955	4.53	12.392
	37/0.5/503 (x = 1.390)	1.08	6.562	2.34	8.290	4.20	12.727
	37/0.5/452 (x = 0.844)	0.72	7.243	1.70	8.970	3.07	13.408
2 group	37/0.5/525 (x = 1.635)	0.15	6.227	1.45	7.955	3.45	12.392
	37/0.5/503 (x = 1.390)	-0.45	6.562	0.82	8.290	2.71	12.727
	37/0.5/452 (x = 0.844)	-0.19	7.243	0.89	8.970	2.43	13.408

TABLE XXVI

2.5 Co 0.3"

	Equivalent square pitch →	8.84"		9.5"		11.02"	
	Cluster type ↓	V_c	y	V_c	y	V_c	y
5 group	90/0.3/580 (x = 2.552)	1.25	5.833	2.68	7.751	4.91	12.678
	90/0.3/525 (x = 1.789)	0.40	6.914	1.71	8.832	3.66	13.759
	90/0.3/485 (x = 1.30)	0.47	7.607	1.53	9.525	3.11	14.452
2 group	90/0.3/580 (x = 2.552)	0.54	5.833	1.88	7.751	4.03	12.678
	90/0.3/525 (x = 1.789)	-0.43	6.914	0.89	8.832	2.92	13.759
	90/0.3/485 (x = 1.30)	-0.55	7.607	0.67	9.525	2.46	14.452

TABLE XXVII

2.5 Co 0.5"

	Equivalent square pitch →	8.84"		9.5"		11.02"	
	Cluster type ↓	V_o	y	V_o	y	V_c	y
5 group	37/0.5/525 (x = 1.635)	0.60	6.227	2.01	7.955	4.16	12.392
	37/0.5/503 (x = 1.390)	0.43	6.562	1.76	8.290	3.73	12.727
	37/0.5/452 (x = 0.844)	0.21	7.243	1.24	8.970	2.69	13.408
2 group	37/0.5/525 (x = 1.635)	-0.78	6.227	0.60	7.955	2.83	12.392
	37/0.5/503 (x = 1.390)	-1.20	6.562	0.16	8.290	2.18	12.727
	37/0.5/452 (x = 0.844)	-0.72	7.243	0.42	8.970	1.80	13.408

5. Conclusions from this study

The following conclusions are based on 5-group calculations for cold, clean systems:-

(i) The void coefficient increases as $y = V_{D_2O}/V_{UO_2}$ is increased. Figure 28 shows that for 0.5" 2.5 Co fuel, which is quite similar to that of the new power reactor

$$\left(\frac{\partial V_c}{\partial y}\right)_x = +0.75\% \qquad \text{approximately}$$

The subscript x indicates that the coefficient is evaluated holding x constant: x and y are made equal to 1.10 and 6.87 respectively, their values for the new power reactor. For this reactor, a 0.5" increase in pitch increases y by 1.074 and therefore increases V_o by 0.81%. A pitch decrease of 0.5" will produce an arithmetically greater change in V_o, since the variation of V_c with y becomes more pronounced as y is reduced.

(ii) The void coefficient increases as $x = V_{H_2O}/V_{UO_2}$ is increased. For 0.5" 2.5 Co fuel

$$\left(\frac{\partial V_c}{\partial x}\right)_y = +0.65\% \qquad \text{approximately}$$

with y=6.87 and x=1.10. It should be stressed that this coefficient is evaluated at constant y and not at constant pitch.

(iii) The void coefficient is insensitive to coolant and moderator temperatures.

(iv) The void coefficient decreases as the enrichment is increased. Figures 24 and 28 show that for 0.5" fuel with x = 1.10 y = 6.87 (the values appropriate to the new power reactor).

$$\frac{\partial V_c}{\partial C_o} = -1.10\% \qquad \text{approximately}$$

(v) The void coefficient decreases slightly as the pin diameter is increased from 0.3" to 0.4", and then increases quite markedly as the diameter is further increased to 0.5".

(vi) The void coefficient is sensitive to fuel disposition, and is minimised by a regular arrangement (except at very wide pitches): close-packing round a central pin produces a greater increase than close-packing up against the pressure tube.

(vii) The void coefficient decreases as the pressure and calandria tube thicknesses are increased.

The predictions (i), (ii), (iii), (iv) and (vii) on the effects of moderator and coolant volume and temperature, and on the effects of enrichment and tube thickness, are in qualitative accord with simple theoretical studies. It seems highly likely that they are qualitatively correct and will be confirmed by experiment and by the use of more detailed theoretical methods: the limited information so far available (3, 12) is encouraging on this point. (The numbers quoted in (i), (ii) and (iv) will no doubt require adjustment).

The predictions (i) to (iv) above are confirmed by the 2-group scheme. This scheme also predicts an increase in V_c as the pin diameter is increased from 0.3" to 0.5": the effect of intermediate pin sizes, of fuel disposition and of tube thickness has not been studied with this scheme.

The 5-group value of V_c is always greater than the 2-group value. The difference is insensitive to x and y, but increases strongly with both enrichment and pin size.

6. Implications for the design of a power reactor

6.0 Present indications are that a design which is relatively simple to engineer and which makes best use of the fuel will have rather too high a void coefficient at the start of life. This section has therefore been written to show how the void coefficient may be reduced. However, if a reactor was found to have too low a void coefficient at any stage of its irradiation history, the remarks below also indicate how the void coefficient might be increased.

6.1 Pitch reduction is the most powerful mechanism for bringing down V_c. This has been known for some time, and the pitch of the new 37-rod power reactor is already at the minimum value fixed by engineering considerations. It seems (16) that this minimum value is not low enough, and that other methods of reducing the total moderating power of the cell must be considered (the theory of sub-section 3.3 makes it clear that this is the overriding criterion). One method of doing this is to increase the calandria tube radius, thus increasing the width of the air gap between the pressure and calandria tubes. Another possibility is the use of displacement tubes in the moderator: these could be flooded if the void coefficient became too negative as irradiation proceeded.

6.2 Reduction of water volume can make a small but useful contribution to the diminution of V_c. However, the calandria tube radius must not be reduced as well, or the resulting increase in bulk moderator volume will nearly cancel the effect of squeezing out light water.

6.3 An increase of enrichment from 2.0 to 2.5 Co will reduce V_c by about 0.5%. Since fuel cost is relatively insensitive to initial enrichment, this method seems worth considering. However, before it could be used a careful examination of the change of V_c with irradiation would be needed.

6.4 If the 5-group scheme is to be believed on this point, the change from the 0.43" pins of the old 61 rod power reactor to the 0.566" pins of the new 37 rod reactor has increased the void coefficient by more than 1% (this increase has been more than compensated by other changes in the design). A reduction of pin size seems to be a possible method of reducing V_c, though it will increase the fuel fabrication charge.

6.5 According to the 5-group scheme it is important to keep the fuel arrangement regular: packing near the pressure tube would be less damaging then packing round the central pin.

6.6 Differential enrichment has often been discussed as a possible method of reducing power peaking in the fuel cluster. Studies by Technical Assessment and Services Division, Winfrith (16) show that a differentially enriched cluster has a higher void coefficient than a uniform cluster of the same mean enrichment. This is to be expected in the light of the arguments presented in this Report, since the fuel of highest enrichment is being placed in the lowest thermal flux, and the mean thermal cross-section of the fuel is reduced by the differential enrichment. From the point of view of this section, the void coefficient could be reduced by differential enrichment, but this would require the most

highly enriched fuel to be placed on the outside of the cluster, and would aggravate the flux peaking.

7. Implications for the specification of an experimental programme

7.0. As far as void coefficient is concerned, the aims of the Water Reactor Physics Division's experimental programme on SGHW are:

(i) To make experiments on cores reasonably similar to that of the new power reactor.

(ii) To demonstrate that SGHW designs with near-zero coefficients are possible.

(iii) To test the general correctness of the predictions of the 5-group scheme, and in particular to compare them with those of the 2-group scheme.

7.1. Since it is a design objective that the void coefficient of the power reactor should be near zero, the first two aims are very similar and we shall discuss them together. The salient parameters of the new 37 rod power reactor are (17):

$x = V_{H_2O}/V_{UO_2} = 1.105$

$y = V_{D_2O}/V_{UO_2} = 6.87$

number of fuel rods/cluster = 37

fuel diameter = 0.566"

fuel enrichment: not specified, but 2.2 Co is a possible value.

canning: zircaloy 0.15" thick

I.D. of pressure tube = 5.14"

It is not possible to mock this up exactly with the materials available at Winfrith at the time of writing (June, 1962). The largest fuel is 0.5" in diameter, and this is available at enrichments of 1.28 Co and 2.5 Co, canned in 0.036" Al in both cases: the latter enrichment is clearly the more suitable for this simulation. Two pressure tubes are available which will accommodate a 37 rod cluster of this fuel. The smaller, with an I.D. of 4.52", gives an x-value of 0.844, which is rather too small; the larger, with an I.D. of 5.25", gives x = 1.635, which is considerably too large. (These values take into account the tie-tubes which, in the experimental assemblies, surround 3 of the fuel rods). Experiments are obviously required in both sizes of pressure tube, with more emphasis on the smaller tube which gives the x-value nearer to that of the power reactor.

7.2. With the lattice plates now available, cores can be built in the sub-critical assemblies SGHW I and SGHW II on the following 3 pitches:

9.5" Δr - equivalent to 8.84" square

9.5" square

11.84" Δr - equivalent to 11.02" square

In the reactor DIMPLE, only the 9.5" square pitch is available. Table XXVIII shows the y values obtained by building 37 rod clusters of 0.5" pins in 4.52" and 5.25" pressure tubes on these pitches.

TABLE XXVIII

Cluster	Pitch	8.84"	9.5"	11.02"
37/0.5/452		7.243	8.970	13.41
37/0.5/525		6.227	7.955	12.39

The table shows that only the two smallest pitches are relevant to a study of the new power reactor, and that with the smaller pressure tube even the smallest pitch is a little too large. The 452 and 525 pressure tubes are normally used with calandria tubes of internal diameters 5.52" and 6.24" respectively. The large (6.24") calandria will be combined with the small pressure tube on the 9.5" triangular pitch to give

$$x = 0.844, \quad y = 6.227$$

These values are both lower than those for the power reactor ($x = 1.105$, $y = 6.87$). This core makes it possible to bracket both the x and y values of the new power reactor, and it has the added advantage that this enlargement of the air gap is (as noted in 6.1) a possible method of reducing V_c in practice.

7.3. It is considered to be very desirable that at least one experiment should be done with values of x and y that are really near to those of the new power reactor (1.10 and 6.87 respectively). A survey of all possible combinations shows that a 43 rod cluster of 0.5" pins in a 5.25" pressure tube on a 9.5" square pitch gives

$$x = 1.20, \quad y = 6.85$$

These are obviously a fair approximation to the power reactor values. The drawbacks of this simulation are that any arrangement of 43 rods in a circular tube is necessarily irregular, and that it will be necessary to use mixed enrichment (1.28 Co and 2.5 Co) to get a core large enough for the measured buckling to

be really accurate. Nonetheless, it is thought that the experiment is well worth making.

7.4. In the fine-structure stack SGHW II, the "coolant" can be heated to 90°C. This will make it possible to confirm the theoretical prediction that V_c is insensitive to coolant temperature.

7.5. A full discussion of the techniques which are being used to check the predictions of the 5-group scheme against experiment, and of the detailed selection of cores for experimental study, will be given elsewhere. However, a comparison of the 5-group and 2-group schemes can best be made on that core for which the difference between them is greatest. A comparison of figures 24 to 28 shows that this core should be constructed with the 2.5 Co 0.5" fuel. An x-value of about 1.4 would maximise the difference, but cannot be achieved with the available pressure tubes: of the tubes now available, the 525 will give slightly the larger difference. Unfortunately, only 1 tonne of the 2.5 Co 0.5" fuel is available, and this is not sufficient to permit the building of a critical assembly of reasonable size in DIMPLE: on the other hand the resulting core is too reactive for sub-critical work at the present stage of the experimental programme. As a compromise, a 90/0.3"/2.5Co/525 core has been chosen as the first loading of DIMPLE, since 2 tonnes of the 2.5 Co 0.3" fuel are available. Although the pin size is rather small, the high enrichment should help in distinguishing between the 2 - and 5 - group schemes.

8. Acknowledgments

We are indebted to Mr. D. A. Newmarch for helpful discussion of the effect of the Dancoff-Ginsburg correction on void coefficient, and to Miss Bridget Manuell for the able and energetic way in which she has handled the very large number of computer runs required for this study.

REFERENCES

1. F. R. ALLEN, D. HICKS and D. C. LESLIE — A 5-group scheme for PTHW physics calculations. AEEW R-105. Commercial

2. A. GREEN — The S.G.H.W. lattice parameter programme. D.E.G. Memo 223(R). (To be published). Commercial (or lower).

3. F. R. ALLEN, A. GREEN, D. C. LESLIE — Theoretical estimates of the void coefficient of the S.G.H.W. reactor. AEEW M-190. Commercial

4. R. A. ALPIAR — SANDPIPER III: a programme to calculate 5-group constants for liquid moderated pressure tube reactors. AEEW R-92 (In preparation). Unclassified.

5. D. C. LESLIE, D. A. NEWMARCH, H. M. BROWN — ARISTOS. A five-group diffusion programme for physics calculations on pressure tube reactors. AEEW R-93. Unclassified.

6. R. A. ALPIAR — METHUSELAH. AEEW R-135. (In preparation). Commercial (or lower).

7. F. R. ALLEN — The effect of design changes on the void coefficient of a 300 MW(E) S.G.H.W. reactor. AEEW M-230. Commercial.

8. D. MOXON — Unpublished.

9. D. MOXON — STAGNANT. A one-dimensional, steady-state, two-group FORTRAN programme for steam generating PTRs. AEEW R-182. Unclassified.

10. J. FELL, G. R. BOLTON, J. RANDLES — An estimate of the stability margin against fundamental mode power oscillations of the S.G.H.W.R. AEEW M-93. Commercial.

11. A. GREEN — Unpublished.

12.	A. J. BRIGGS	To be published.
13.	D. HICKS	Resonance escape in hydrogenous moderated systems. AEEW M-101. Not for publication.
14.	L. DRESNER	Resonance absorption in nuclear reactors. Pergamon Press, 1960.
15.	W. ROTHENSTEIN	Collision probabilities and resonance integrals for lattices. Nuc. Sci. and Eng. 7, 162 (1960).
16.	D. HICKS	To be published.
17.	N. BRADLEY	Unpublished information.

APPENDIX

Deduction of some formulae cited in Section 4

In the 5-group scheme,

$$k_\infty = (\eta f)_t p + (\eta f)_f (1-p) \qquad (A.1)$$

Ignoring the variation of and with , we have

$$\frac{\partial k_\infty}{\partial y} = \{(\eta f)_t - (\eta f)_f\} \frac{\partial p}{\partial y}$$

Then from the definition of void coefficient given in equation (2.1)

$$\frac{\partial V_c}{\partial y} = 100 \{(\eta f)_t - (\eta f)_f\} \frac{\partial p}{\partial y} \Big|_{\rho=0.8}^{\rho=0.4} \qquad (A.2)$$

Now the "p" cited in equation (A.1) is actually the non-capture probability in the whole of the fast group. However the variation of this quantity with y is very similar to that of p_3, the escape probability in group 3. From the formulae given in sub-section 3.3, we have

$$p_3 = \frac{0.836(x\rho + y) - 0.46\sigma_{3a}}{0.836(x\rho+y) + 0.54\sigma_{3a}} \qquad (A.3)$$

(epithermal capture in U-235 being ignored). From (A.3)

$$\frac{\partial p_3}{\partial y} = \frac{0.836\sigma_{3a}}{\{0.836(x\rho+y) + 0.54\sigma_{3a}\}^2}$$

whence equation (4.1) follows at once.

The variation of V_c with x can be dealt with in the same sort of way, although the variation of $(\eta f)_t$ with x cannot be neglected. We have

$$\frac{\partial V_c}{\partial x} = 100 \left[\{(\eta f)_t - (\eta f)_f\} \frac{\partial p}{\partial x} + p \frac{\partial (\eta f)_t}{\partial x} \right]_{\rho=0.8}^{\rho=0.4}$$

$$= 100 \left[\{(\eta f)_t - (\eta f)_f\} \frac{0.836\rho\sigma_{3a}}{\{0.836(x\rho+y) + 0.54\sigma_{3a}\}^2} + p \frac{\partial (\eta f)_t}{\partial x} \right]_{\rho=0.8}^{\rho=0.4}$$

by arguments identical with those used above. Now from equation (3.3) f_t may be written

$$\frac{1}{f_t} - 1 = \alpha x \rho + \beta \qquad (A.4)$$

α and β being constants [if we ignore the variation of Σ_{t5} with x, which implies that we should also ignore the variation of $(\eta_5)_t$]. From (A.4)

$$\frac{\partial f_t}{\partial x} = -\alpha\rho f_t^2$$

from which equation (4.2) follows.

VARIATION OF ηf AND p FOR THE 37/0·5/2·5/452/9·5" LATTICE ACCORDING TO THE 2 AND 5 GROUP SCHEMES

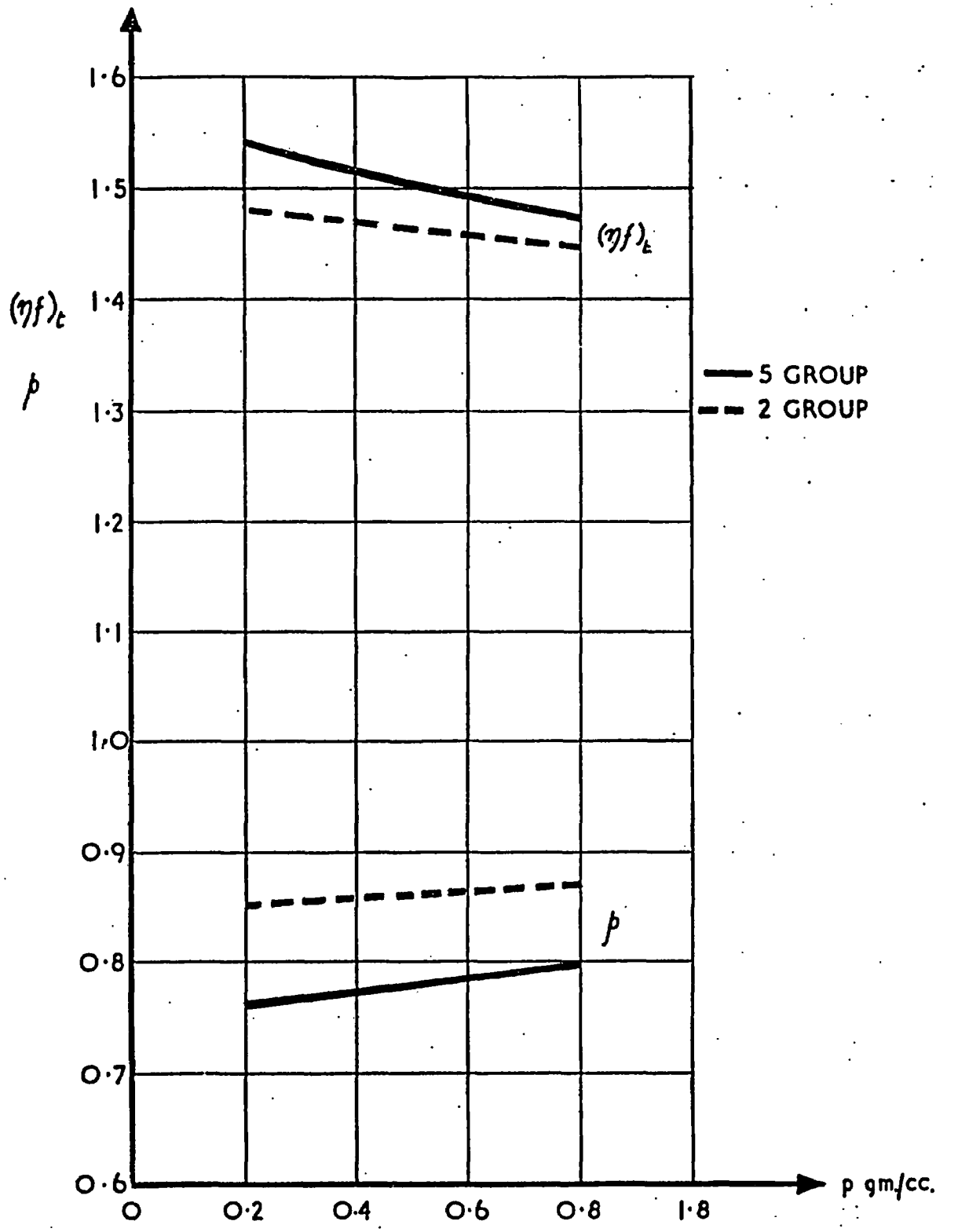

FIGURE 1

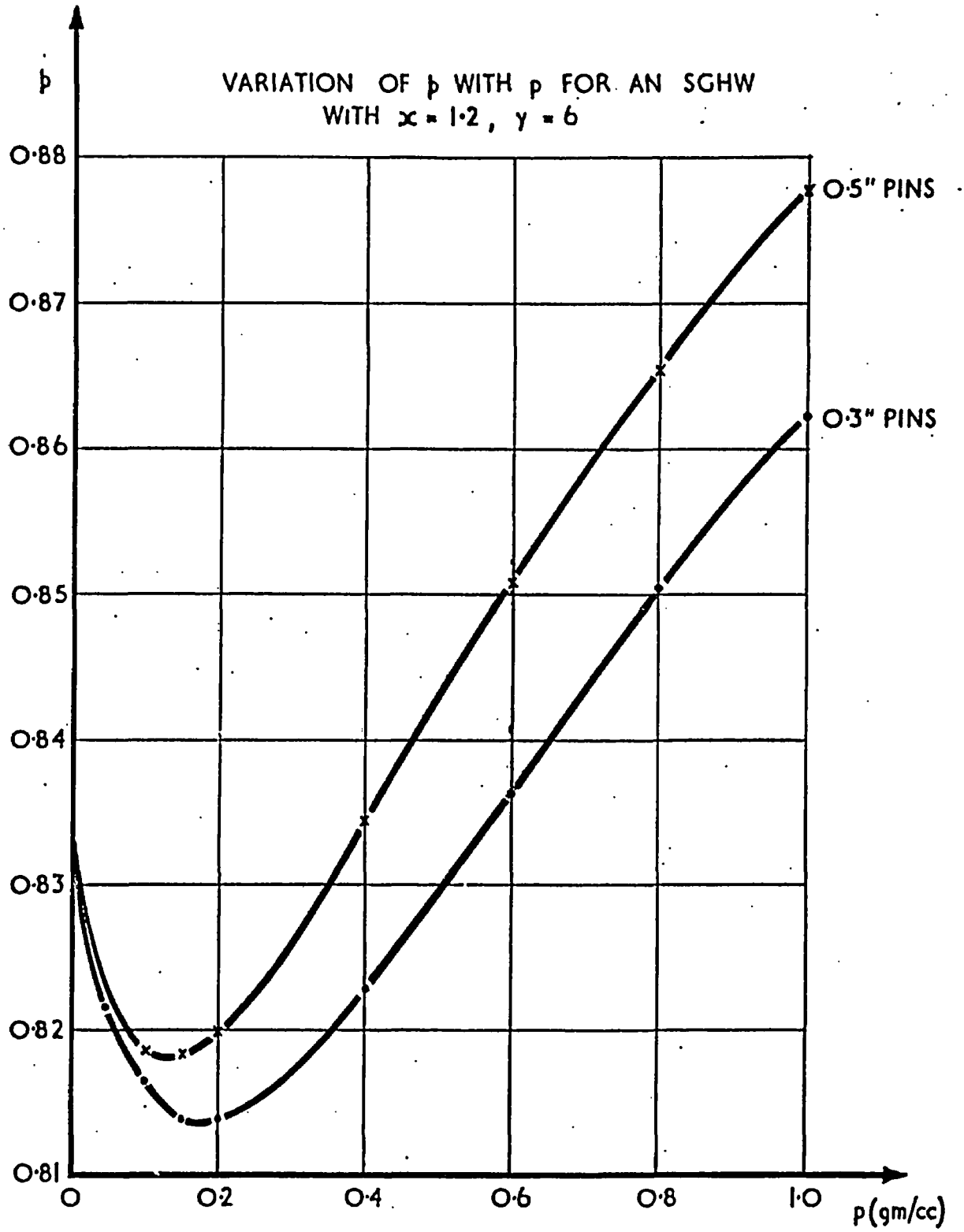
VARIATION OF þ WITH p FOR AN SGHW
WITH x = 1·2 , y = 6
þ
0·88
0·87
0·86
0·85
0·84
0·83
0·82
0·81
0
0·2
0·4
0·6
0·8
1·0
p(gm/cc)
0·5" PINS
0·3" PINS

FIGURE 2

VARIATION OF VOID COEFFICIENT WITH MODERATOR TO FUEL RATIO FOR THE 37/0·5/2·5/452 LATTICE ACCORDING TO THE 5 & 2-GROUP SCHEMES

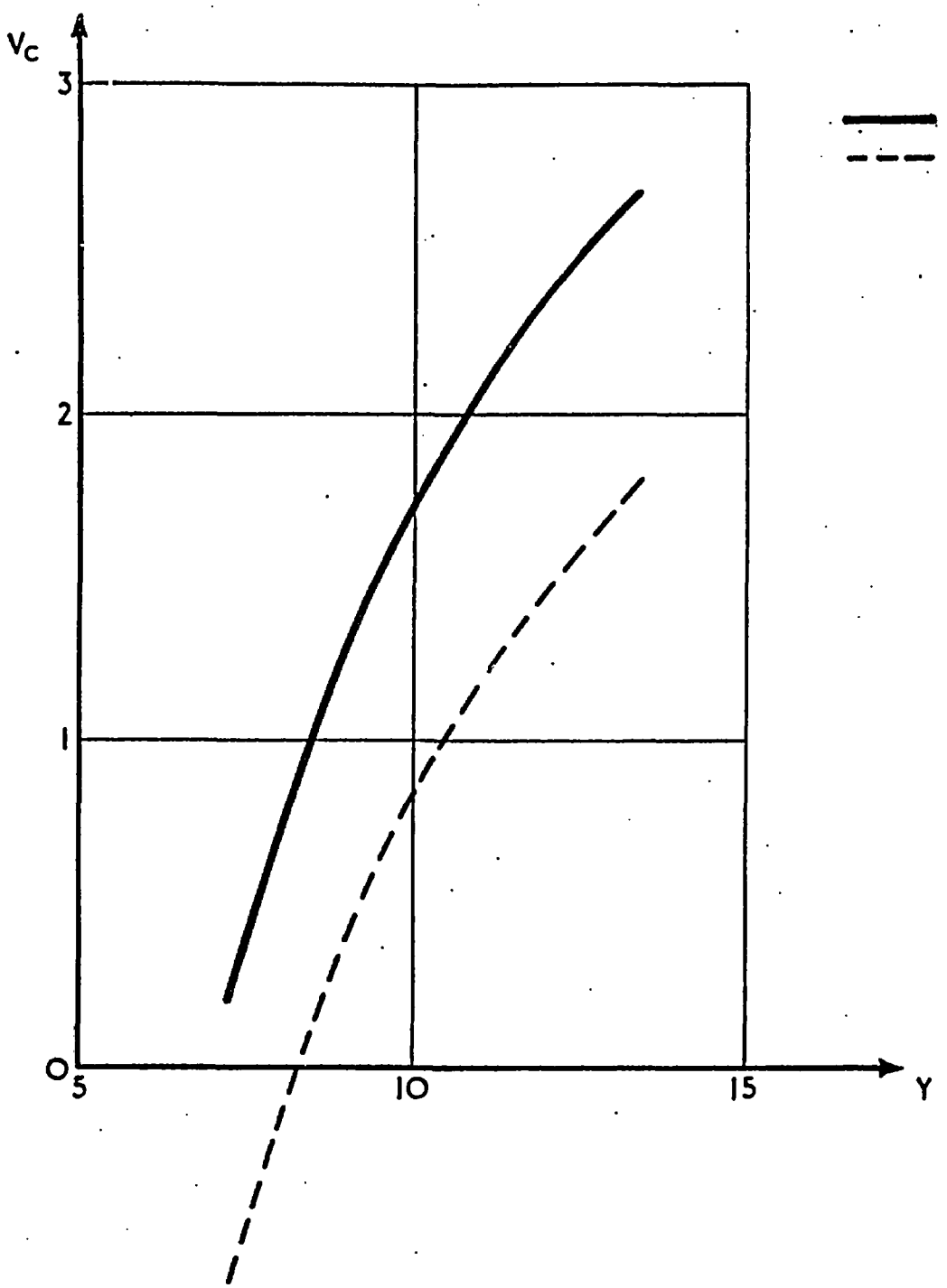

FIGURE 3

VARIATION OF VOID COEFFICIENT WITH COOLANT TO FUEL VOLUME RATIO FOR THE 37/0·5/ 2·5C_o CLUSTER IN VARIOUS PRESSURE TUBES; AS GIVEN BY THE 5 GROUP SCHEME.

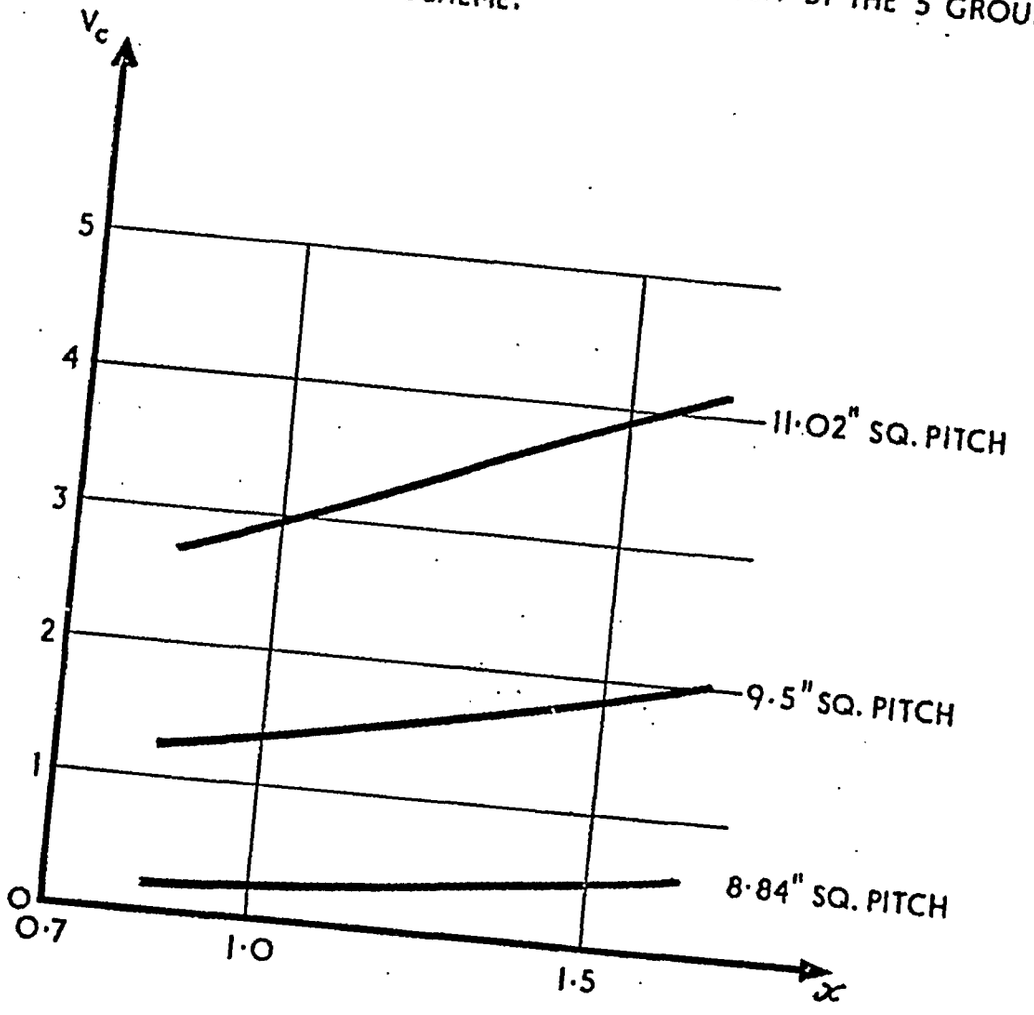

FIGURE 4

VARIATION OF VOID COEFFICIENT WITH COOLANT TO FUEL VOLUME RATIO FOR THE 37/0·5/2·5C_o CLUSTER, AS GIVEN BY THE 5-GROUP SCHEME.

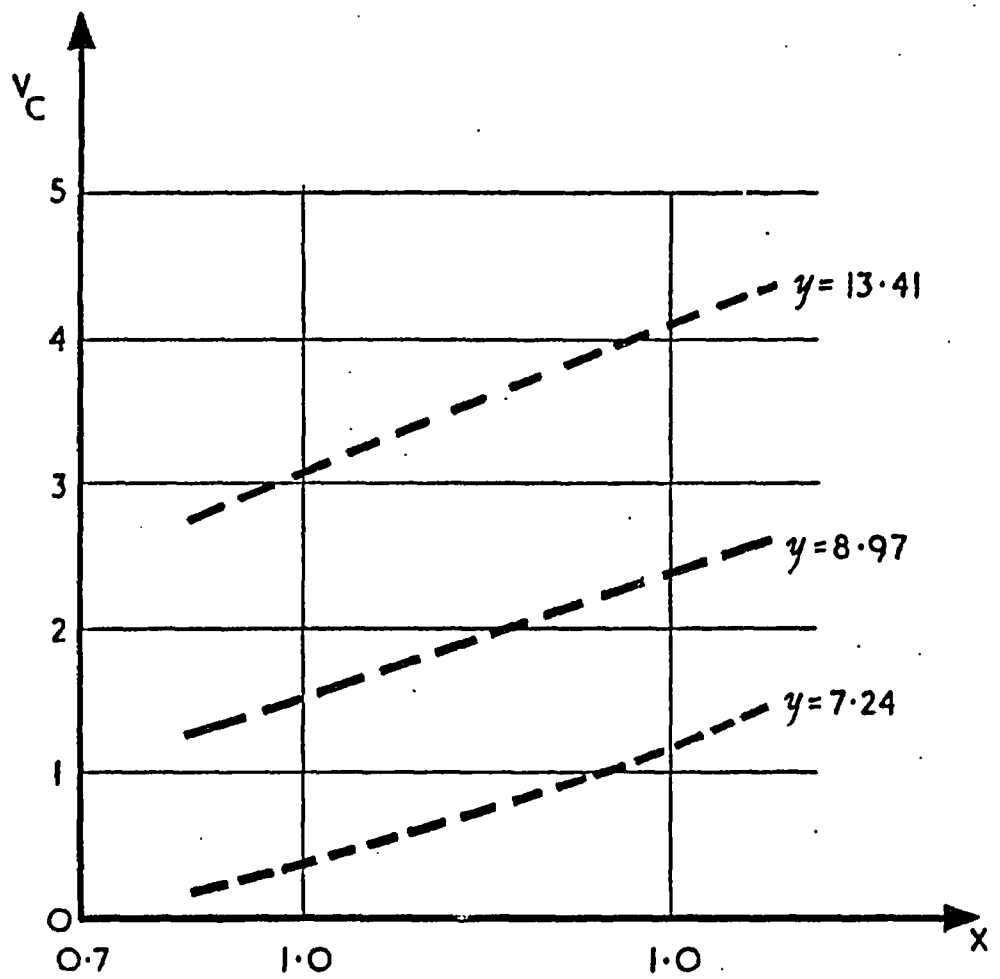

FIGURE 5

VARIATION OF VOID COEFFICIENT WITH COOLANT TO FUEL VOLUME RATIO FOR THE 37/0·5/1·28 C_o LATTICES AS GIVEN BY THE 5-GROUP SCHEME.

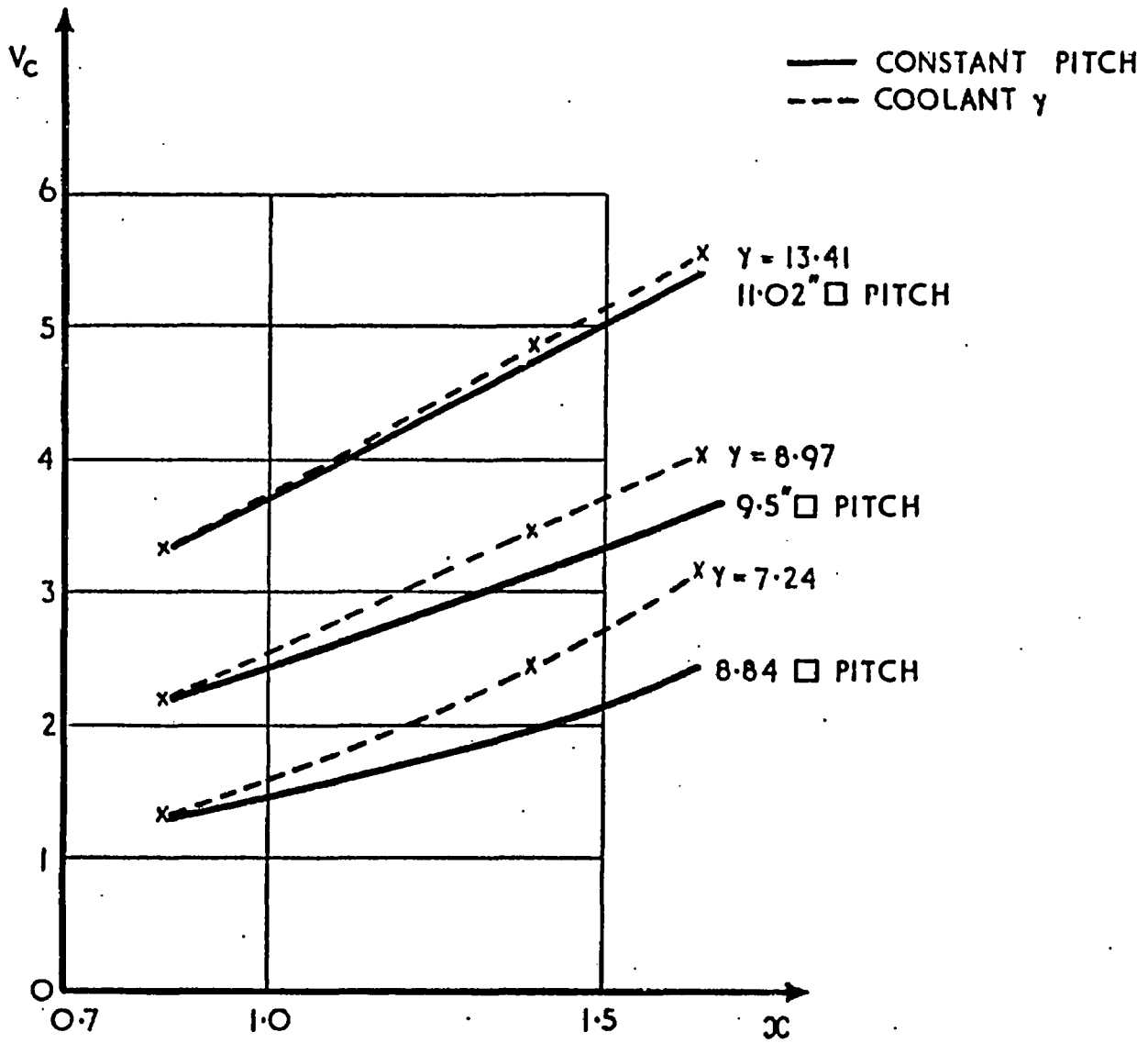

FIGURE 6

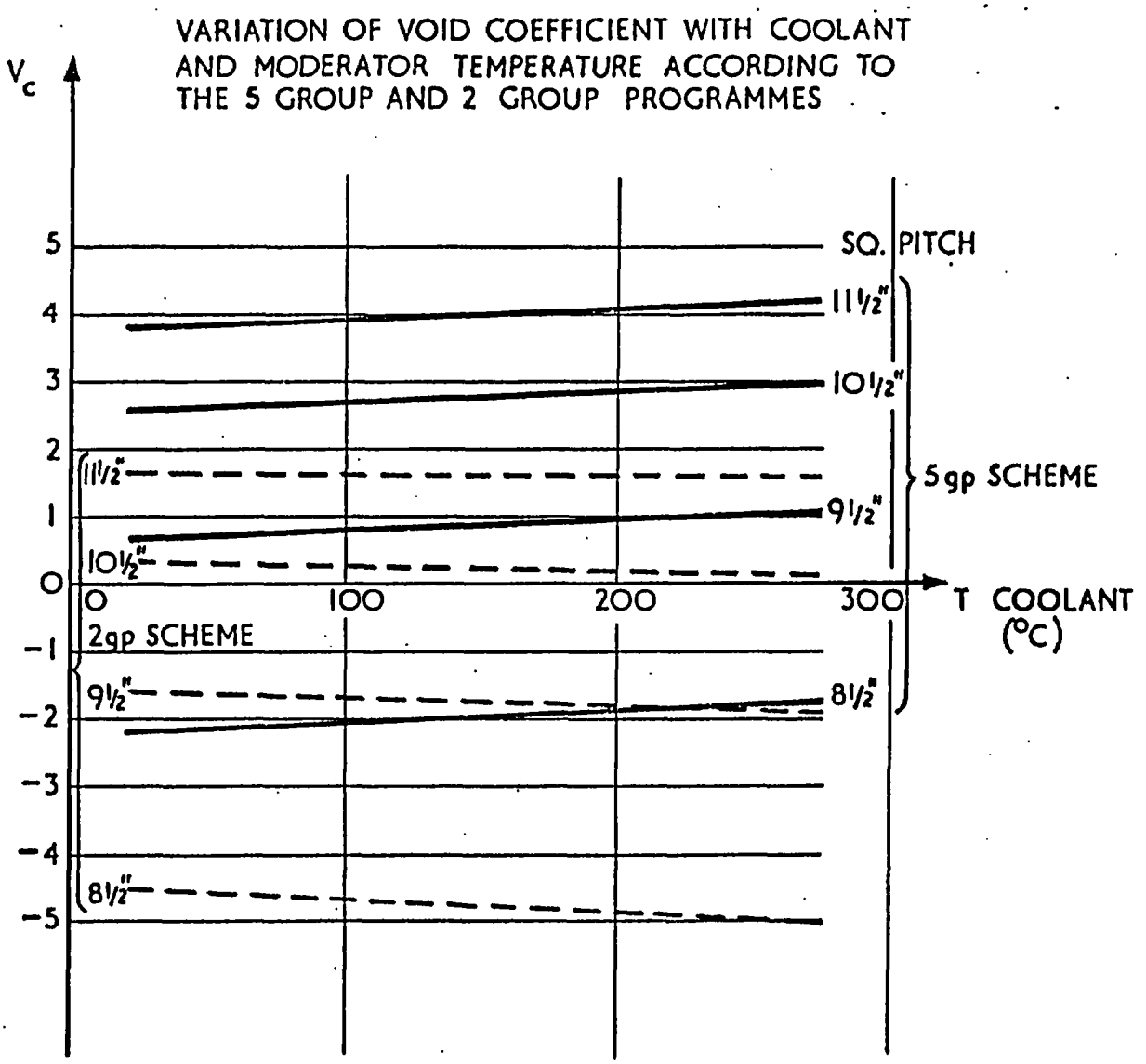
VARIATION OF VOID COEFFICIENT WITH COOLANT AND MODERATOR TEMPERATURE ACCORDING TO THE 5 GROUP AND 2 GROUP PROGRAMMES
V_c
5
4
3
2
1
0
−1
−2
−3
−4
−5
0
100
200
300
T COOLANT (°C)
SQ. PITCH
11½"
10½"
9½"
8½"
5gp SCHEME
2gp SCHEME

FIGURE 7

VARIATION OF VOID COEFFICIENT WITH ENRICHMENT ACCORDING TO THE 5-GROUP SCHEME, FOR THE 37/0·5/503 LATTICE

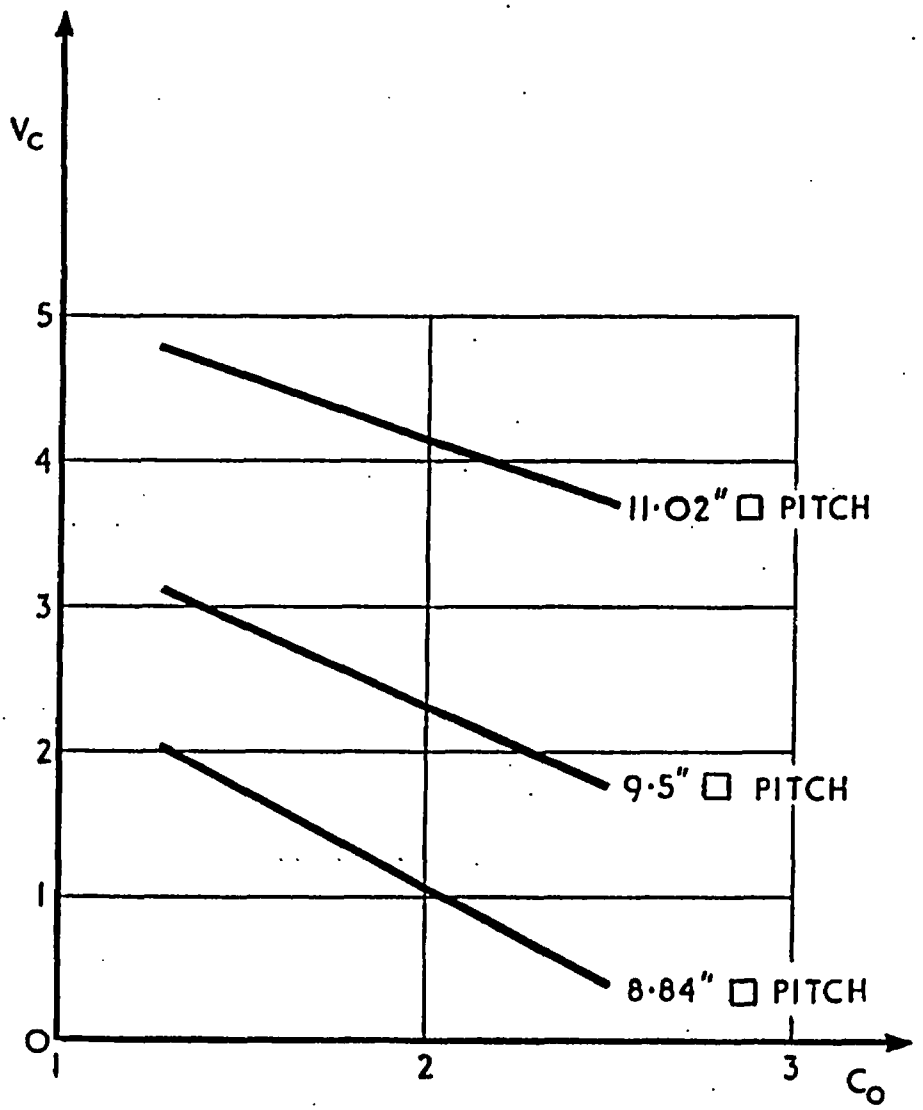

FIGURE 8

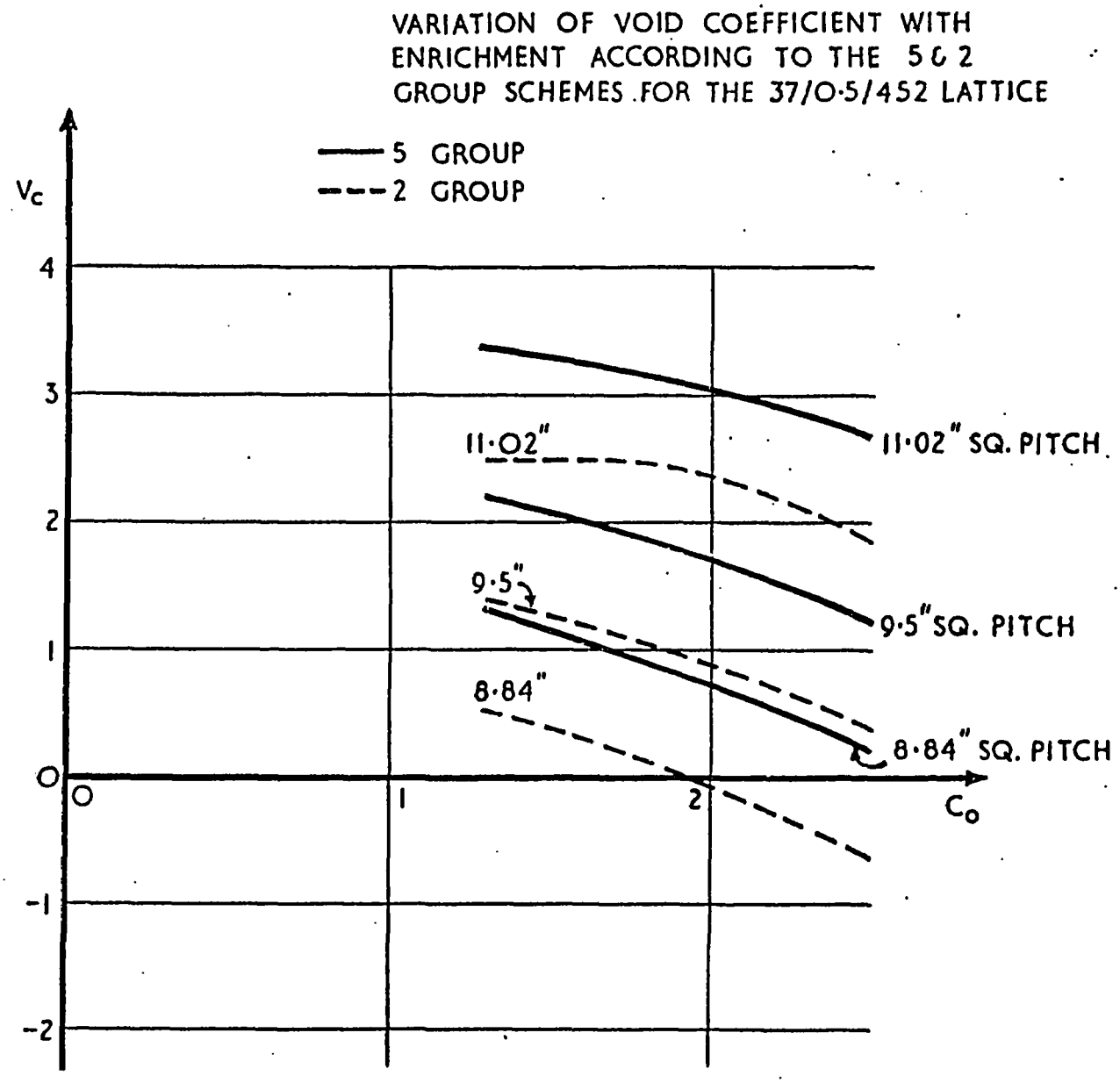
VARIATION OF VOID COEFFICIENT WITH ENRICHMENT ACCORDING TO THE 5 & 2 GROUP SCHEMES FOR THE 37/0·5/452 LATTICE
5 GROUP
2 GROUP
Vc
4
3
2
1
0
-1
-2
0
1
2
Co
11·02"
11·02" SQ. PITCH
9·5"
9·5" SQ. PITCH
8·84"
8·84" SQ. PITCH

FIGURE 9

VARIATION OF VOID COEFFICIENT WITH ENRICHMENT ACCORDING TO BOTH SCHEMES FOR THE 90/0·3/5·25 LATTICE

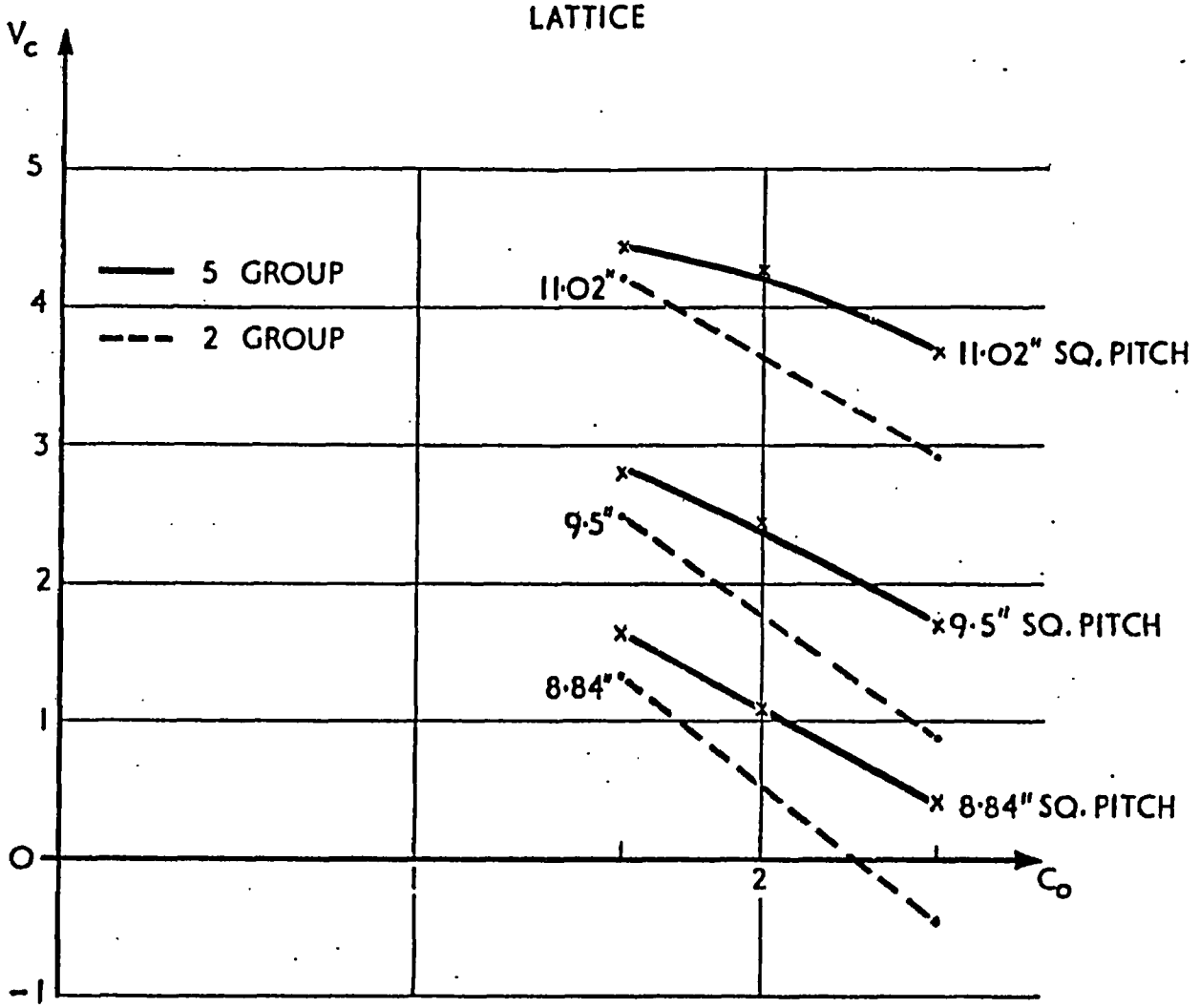

FIGURE 10

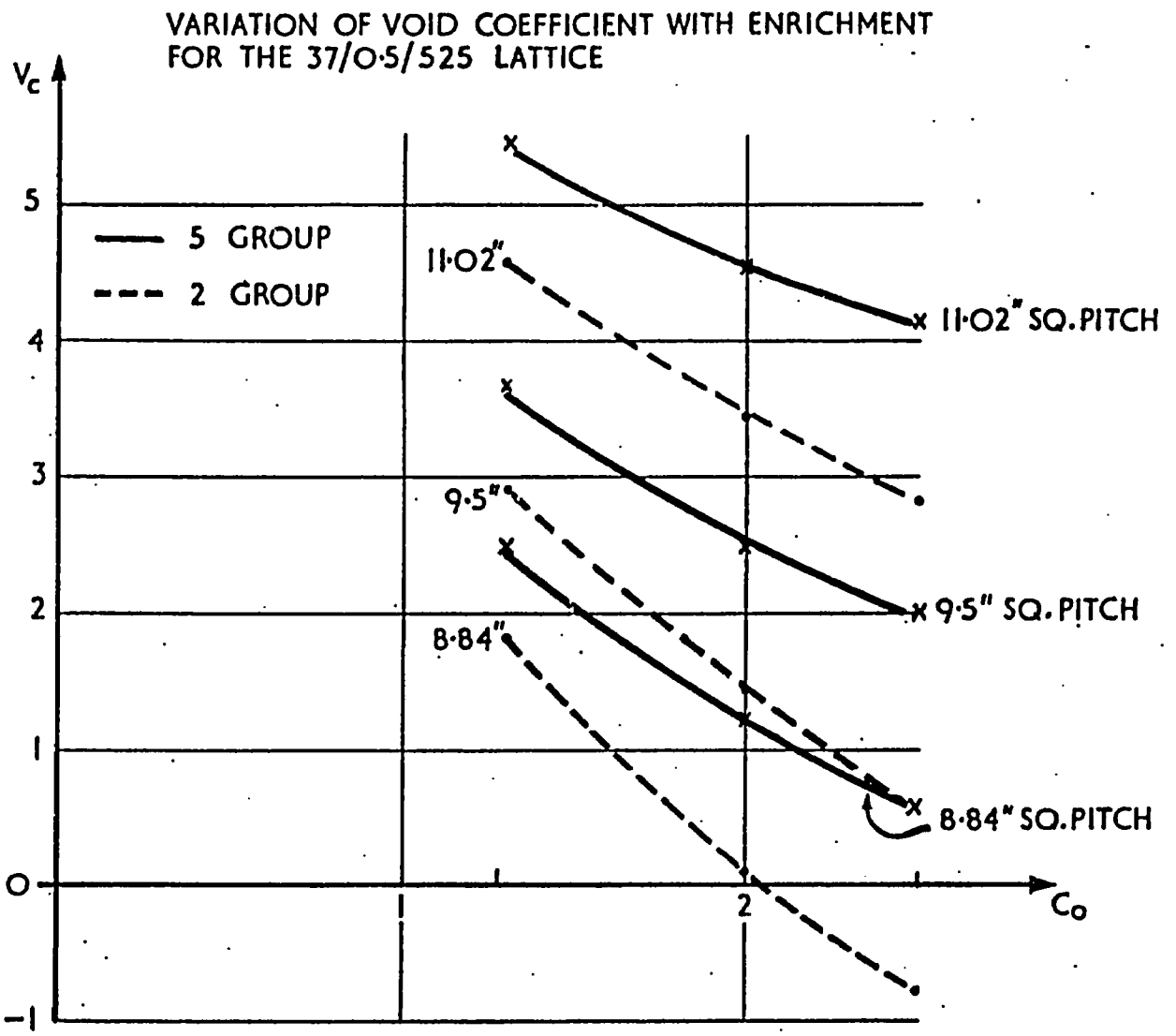
VARIATION OF VOID COEFFICIENT WITH ENRICHMENT
FOR THE 37/0·5/525 LATTICE
V_c
5
4
3
2
1
0
−1
5 GROUP
2 GROUP
11·02"
9·5"
8·84"
11·02" SQ. PITCH
9·5" SQ. PITCH
8·84" SQ. PITCH
2
C_o

FIGURE 11

VARIATION OF VOID COEFFICIENT WITH PIN SIZE FOR THE 37, 61 AND 91 ROD LATTICES AT 2 C_o AND 2·5 C_o ACCORDING TO THE 5 GROUP SCHEME.

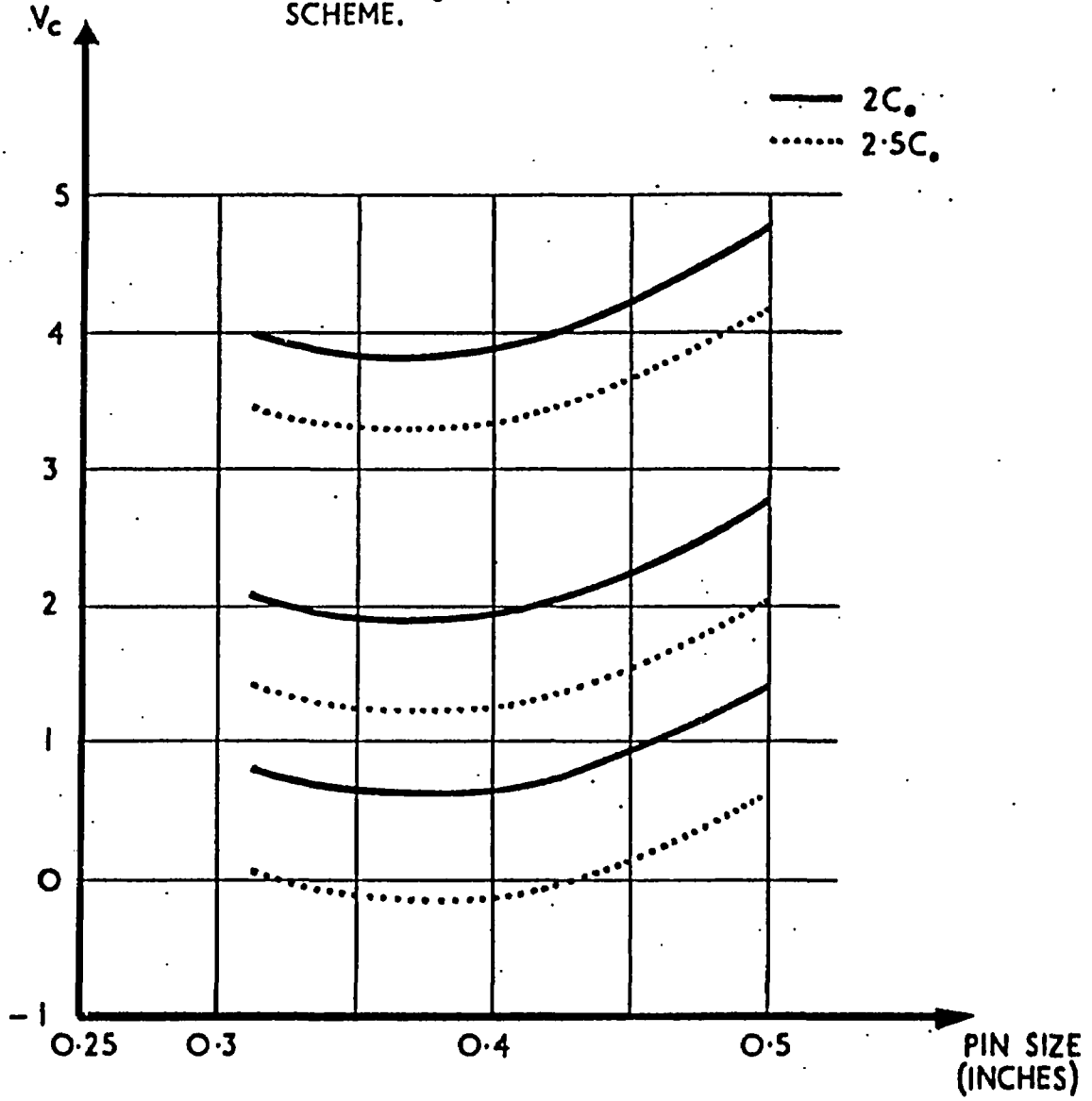

FIGURE 12

ILLUSTRATION OF THE CLOSE-PACKED, NORMAL AND EDGE-PACKED FUEL REGIONS FOR THE 37/0·5/525 LATTICE CELL (PINS NOT TO SCALE)

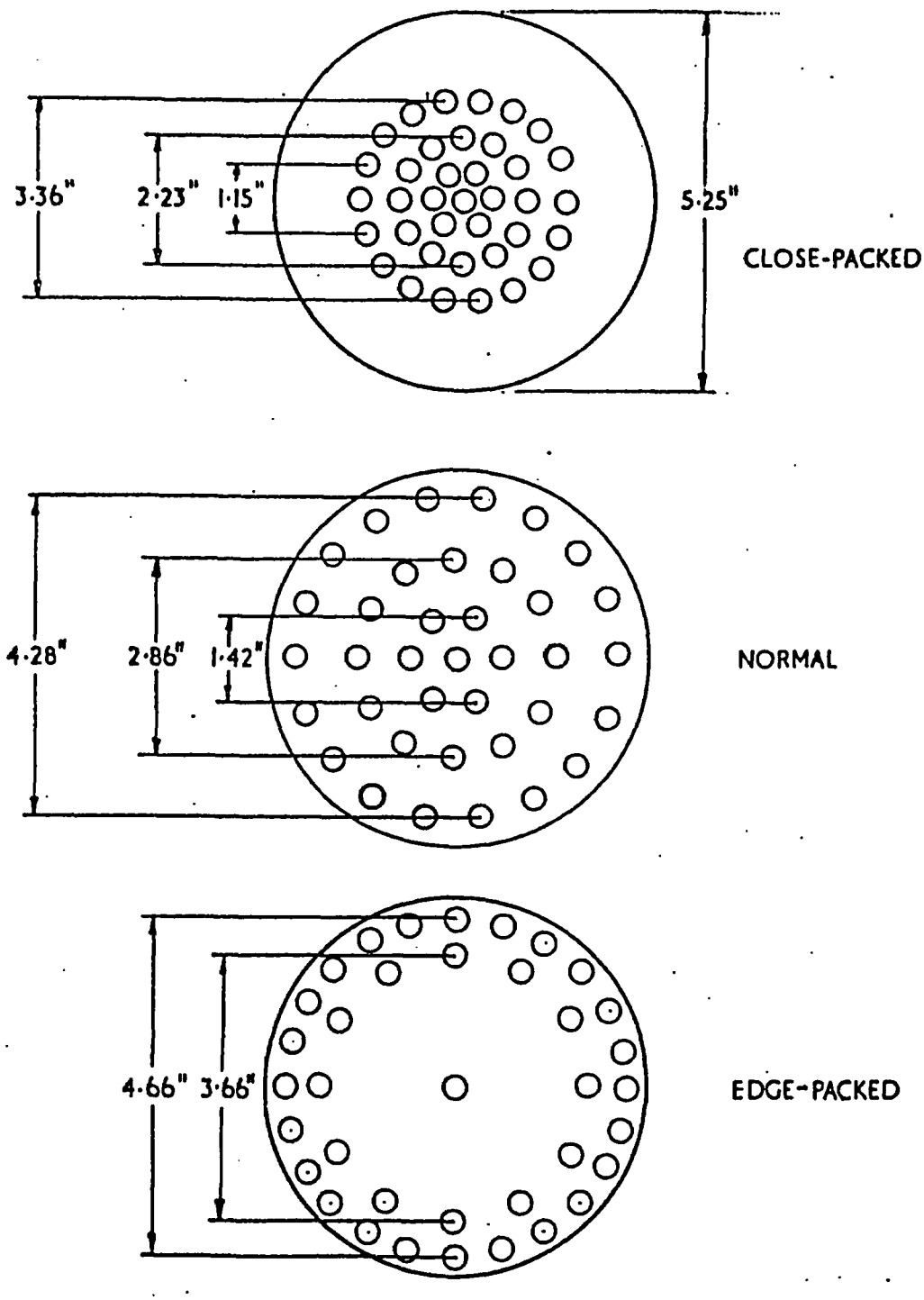

FIGURE 13

VARIATION OF VOID COEFFICIENT WITH y
FOR THE 1·28 C_o, 0·5" DIAMETER FUEL,
ACCORDING TO THE 5-GROUP SCHEME

1·28 C_o, 0·5"

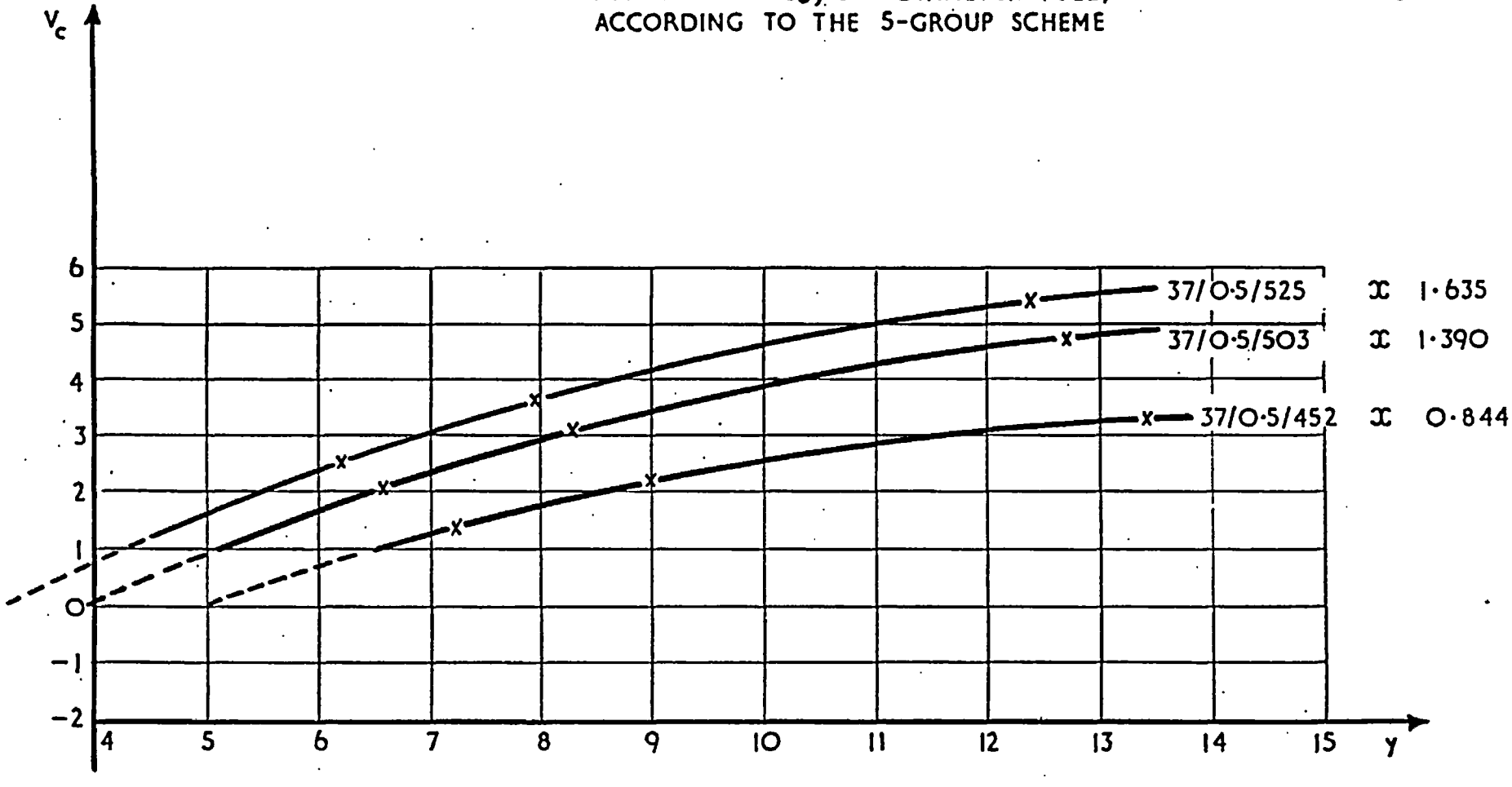

FIGURE 14

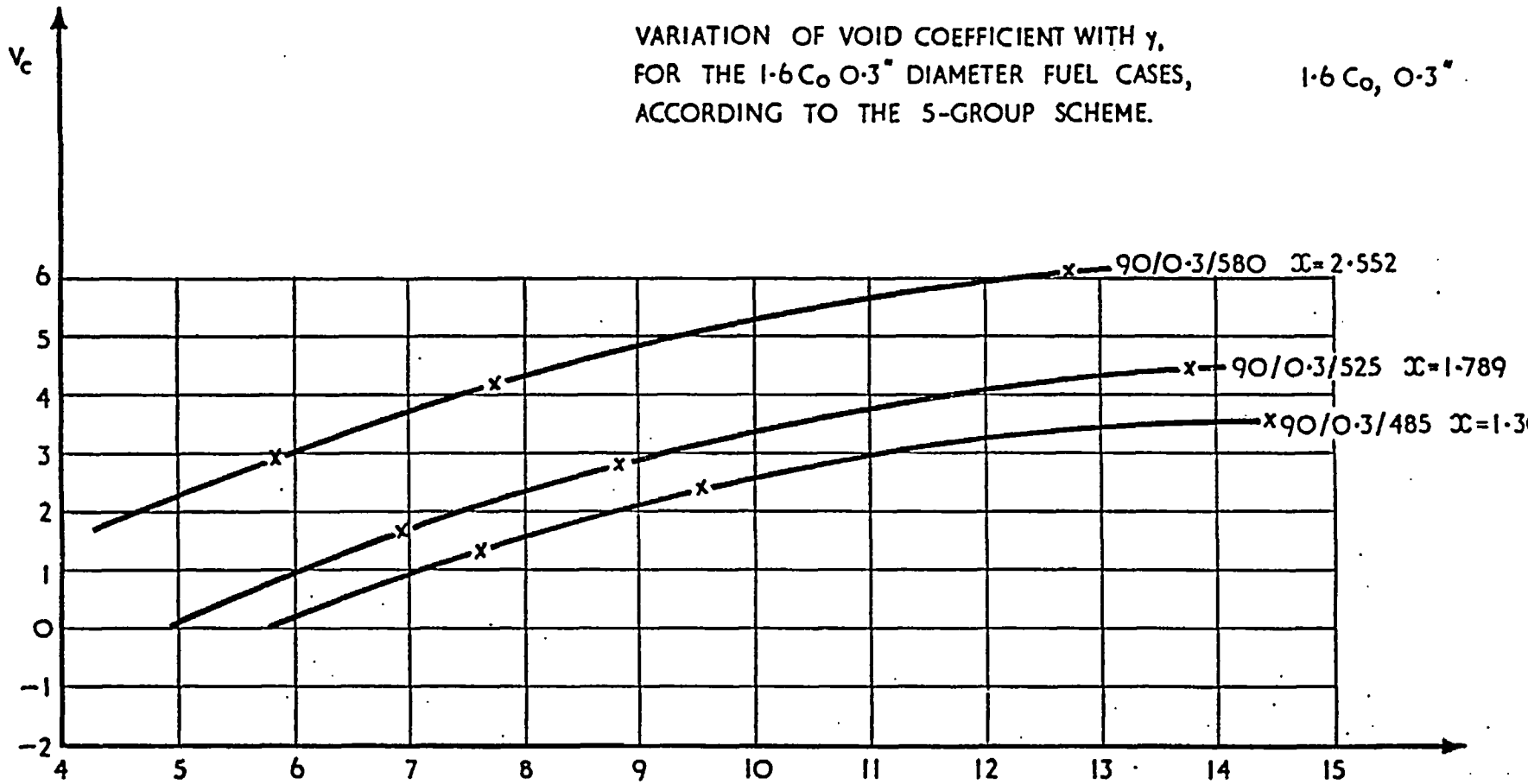
VARIATION OF VOID COEFFICIENT WITH y,
FOR THE 1·6 Co 0·3" DIAMETER FUEL CASES,
ACCORDING TO THE 5-GROUP SCHEME.
1·6 Co, 0·3"
Vc
90/0·3/580 x= 2·552
90/0·3/525 x=1·789
90/0·3/485 x=1·30
6
5
4
3
2
1
0
−1
−2
4
5
6
7
8
9
10
11
12
13
14
15

FIGURE 15

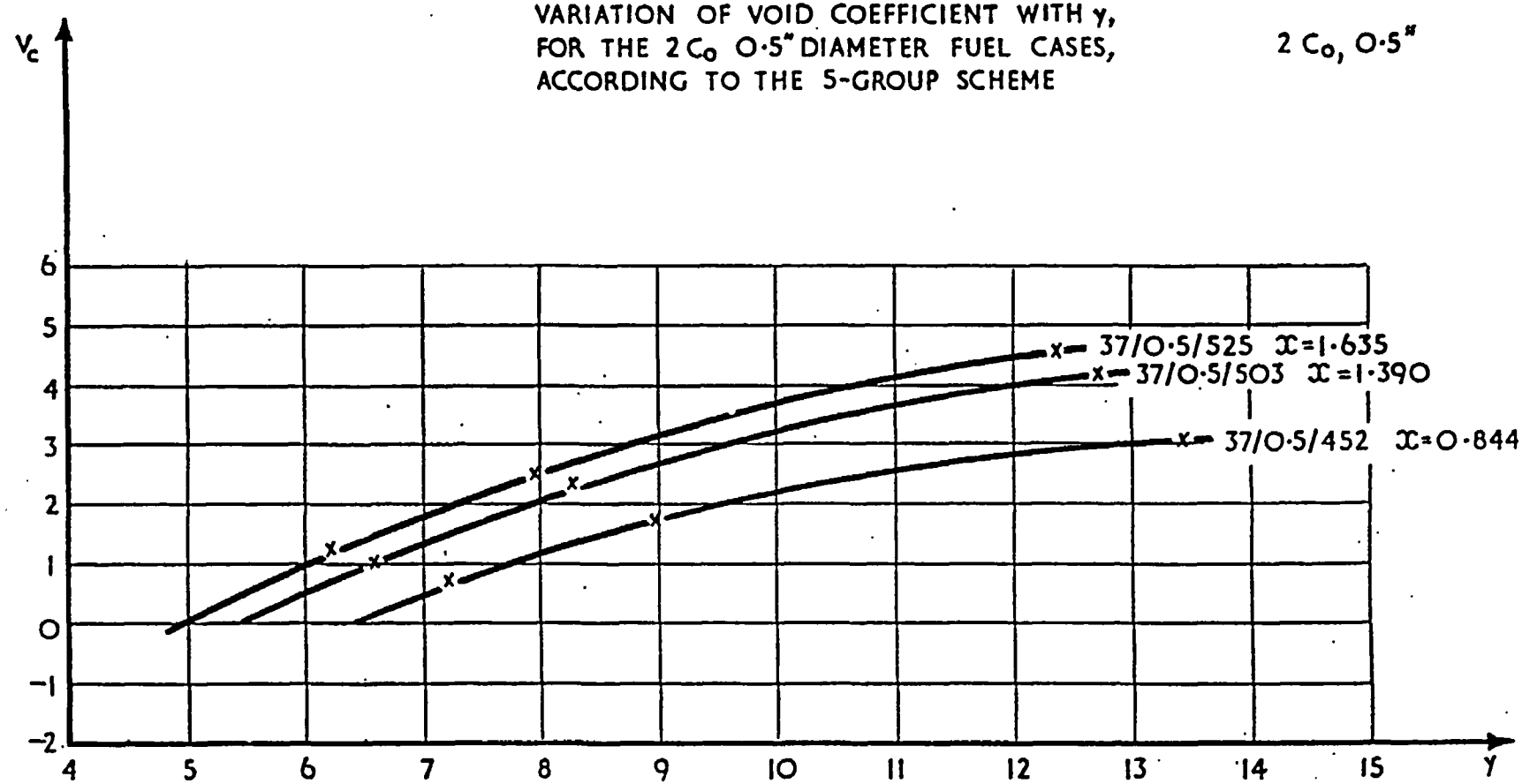
VARIATION OF VOID COEFFICIENT WITH y,
FOR THE 2 Co 0·5" DIAMETER FUEL CASES,
ACCORDING TO THE 5-GROUP SCHEME
2 Co, 0·5"
Vc
6
5
4
3
2
1
0
−1
−2
4
5
6
7
8
9
10
11
12
13
14
15
y
37/0·5/525 𝔵=1·635
37/0·5/503 𝔵=1·390
37/0·5/452 𝔵=0·844

FIGURE 16

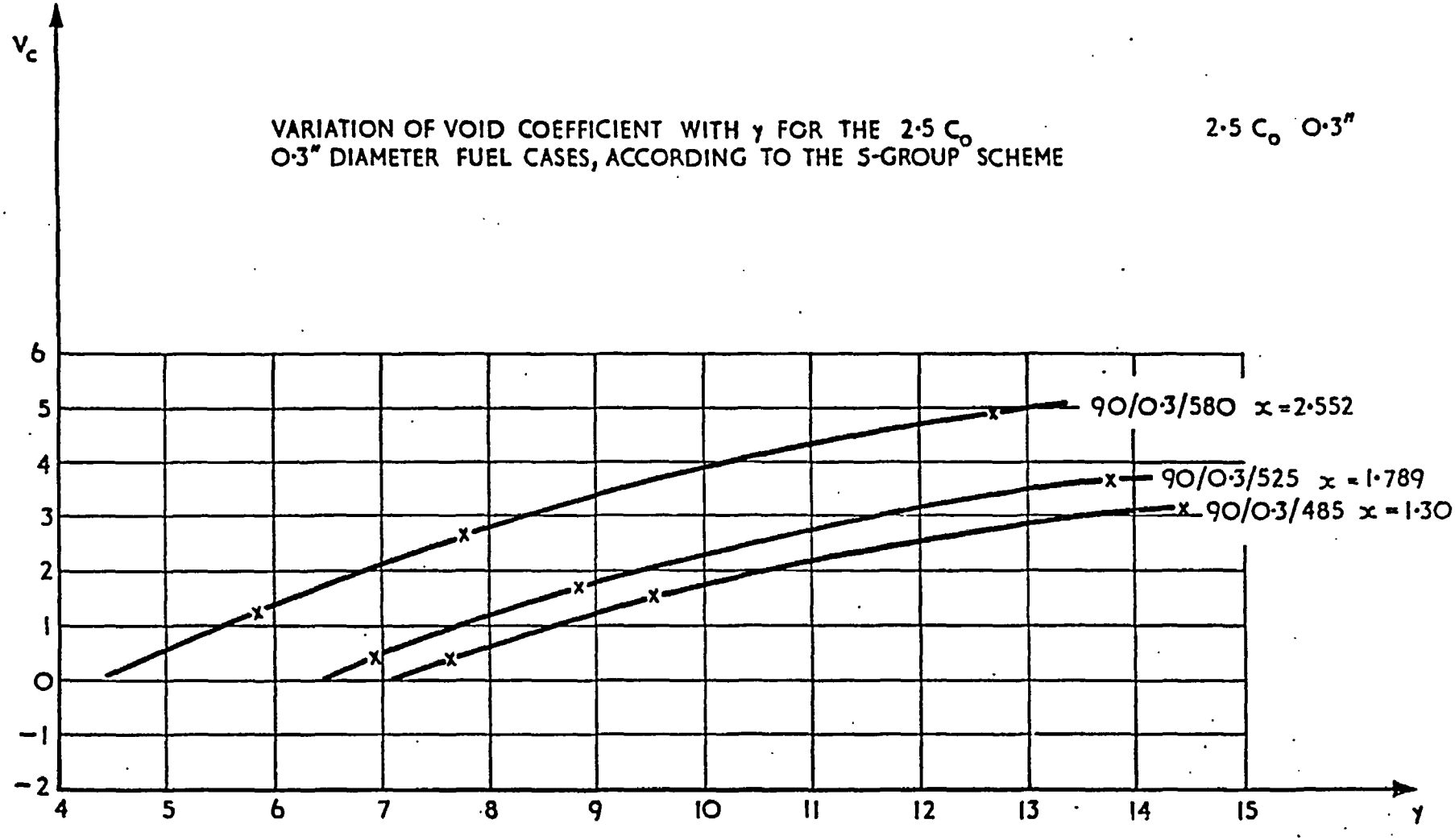
VARIATION OF VOID COEFFICIENT WITH y FOR THE 2·5 C₀ 0·3" DIAMETER FUEL CASES, ACCORDING TO THE 5-GROUP SCHEME
2·5 C₀ 0·3"
Vc
6
5
4
3
2
1
0
−1
−2
4
5
6
7
8
9
10
11
12
13
14
15
y
90/0·3/580 x = 2·552
90/0·3/525 x = 1·789
90/0·3/485 x = 1·30

FIGURE 17

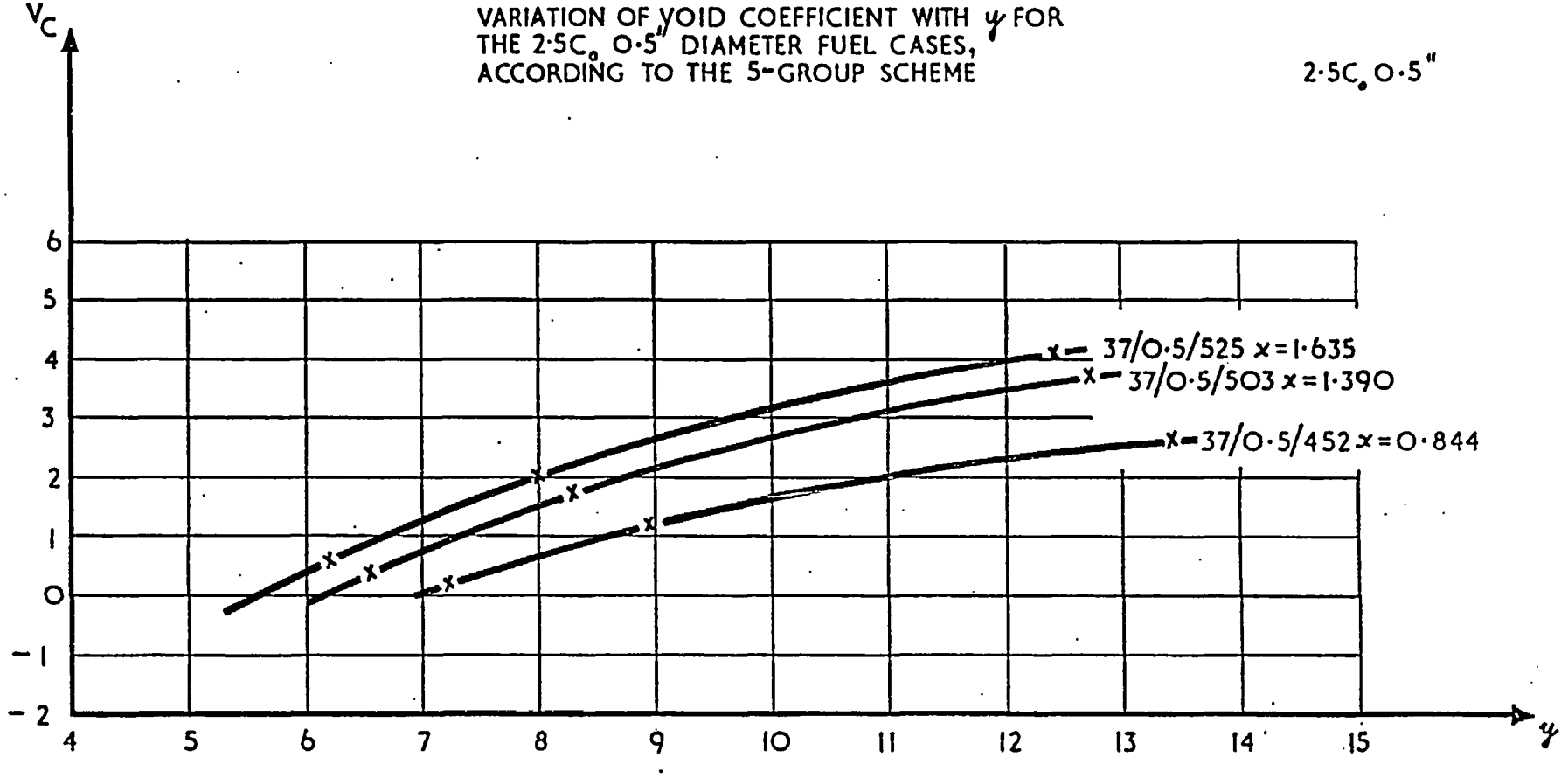
VARIATION OF VOID COEFFICIENT WITH ψ FOR THE 2·5C₀ 0·5" DIAMETER FUEL CASES, ACCORDING TO THE 5-GROUP SCHEME
2·5C₀ 0·5"
V_C
6
5
4
3
2
1
0
−1
−2
4
5
6
7
8
9
10
11
12
13
14
15
ψ
37/0·5/525 x = 1·635
37/0·5/503 x = 1·390
37/0·5/452 x = 0·844

FIGURE 18

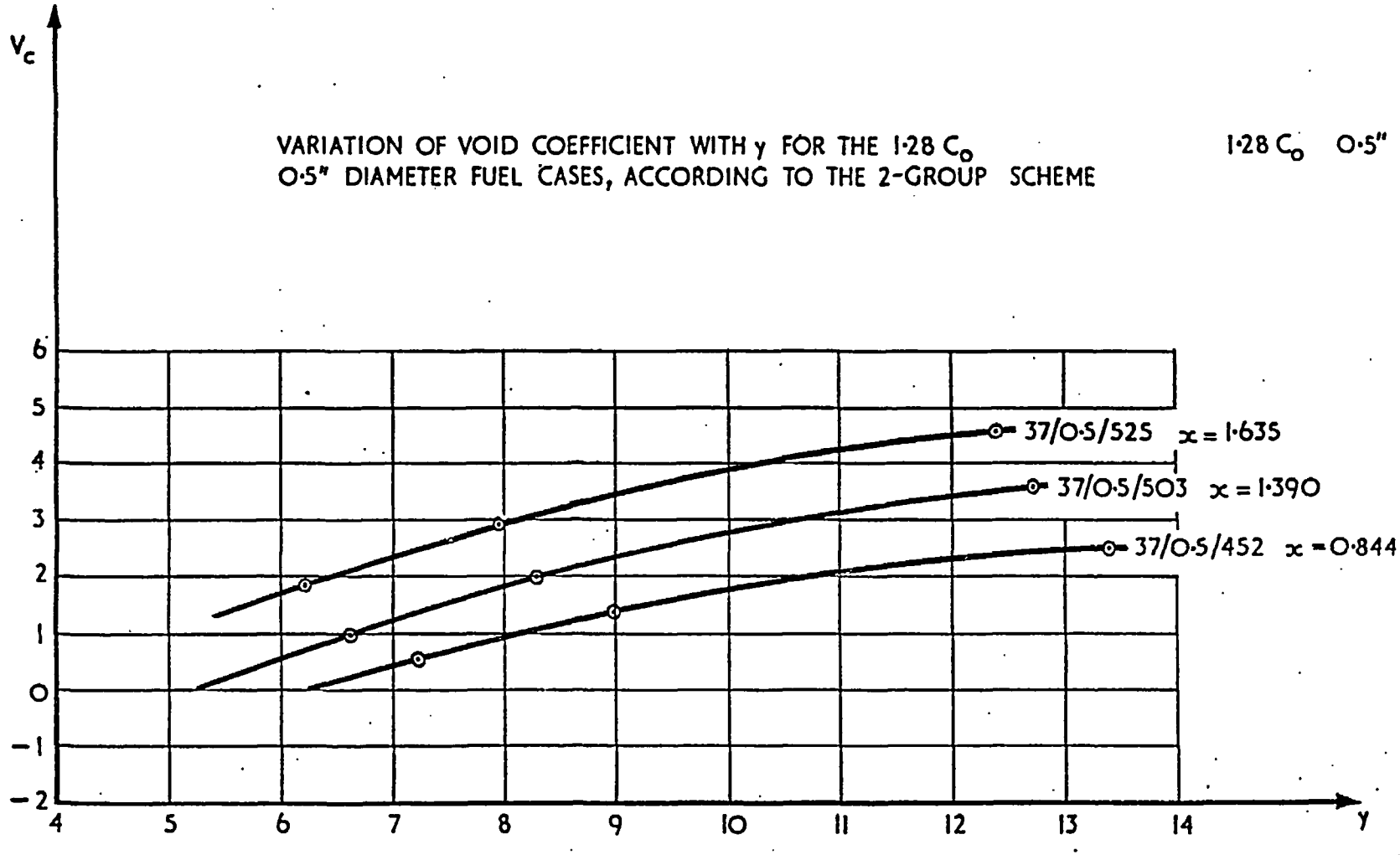
V_c
VARIATION OF VOID COEFFICIENT WITH y FOR THE 1·28 C_o
0·5" DIAMETER FUEL CASES, ACCORDING TO THE 2-GROUP SCHEME
1·28 C_o 0·5"
6
5
4
3
2
1
0
−1
−2
4
5
6
7
8
9
10
11
12
13
14
y
37/0·5/525 x = 1·635
37/0·5/503 x = 1·390
37/0·5/452 x = 0·844

FIGURE 19

VARIATION OF VOID COEFFICIENT WITH y, FOR THE 1·6 C_o 0·3" DIAMETER FUEL CASES, ACCORDING TO THE 2 GROUP SCHEME.

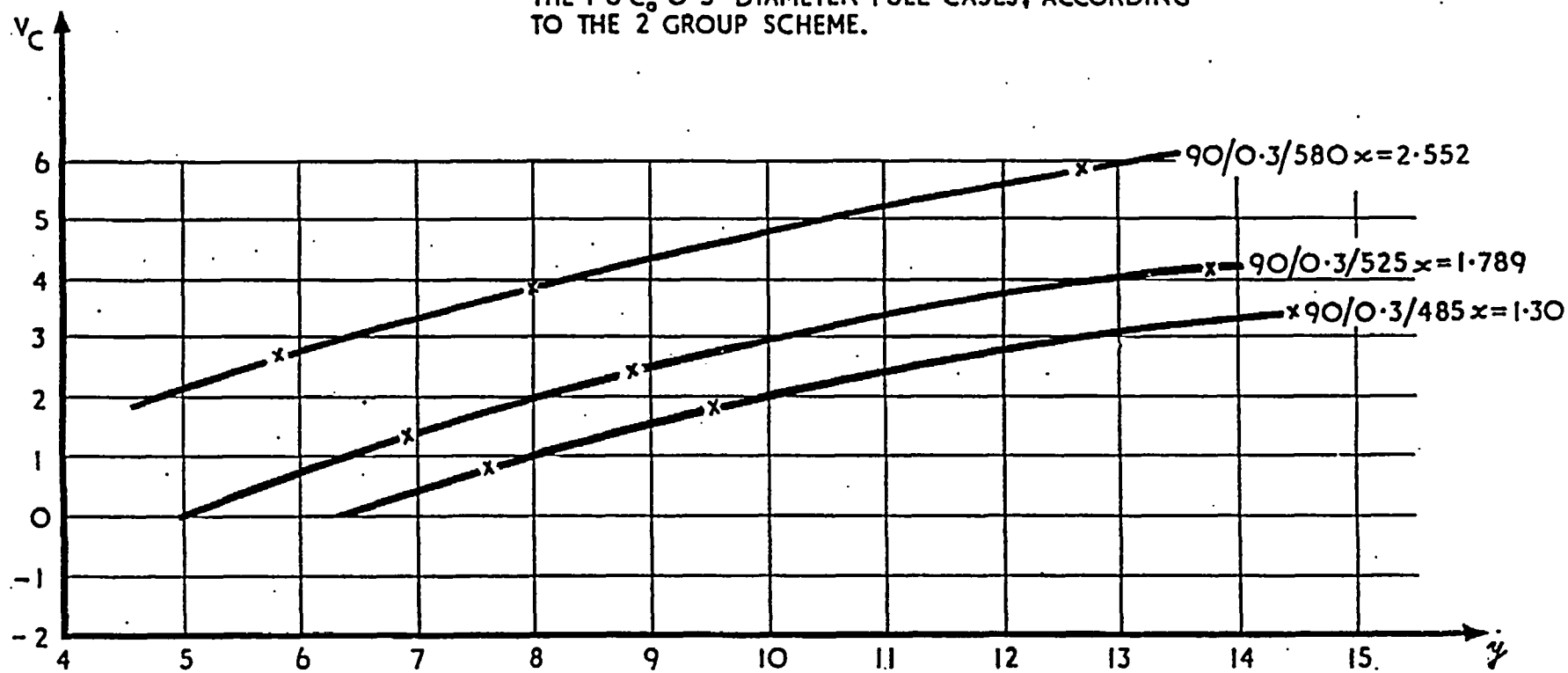

FIGURE 20

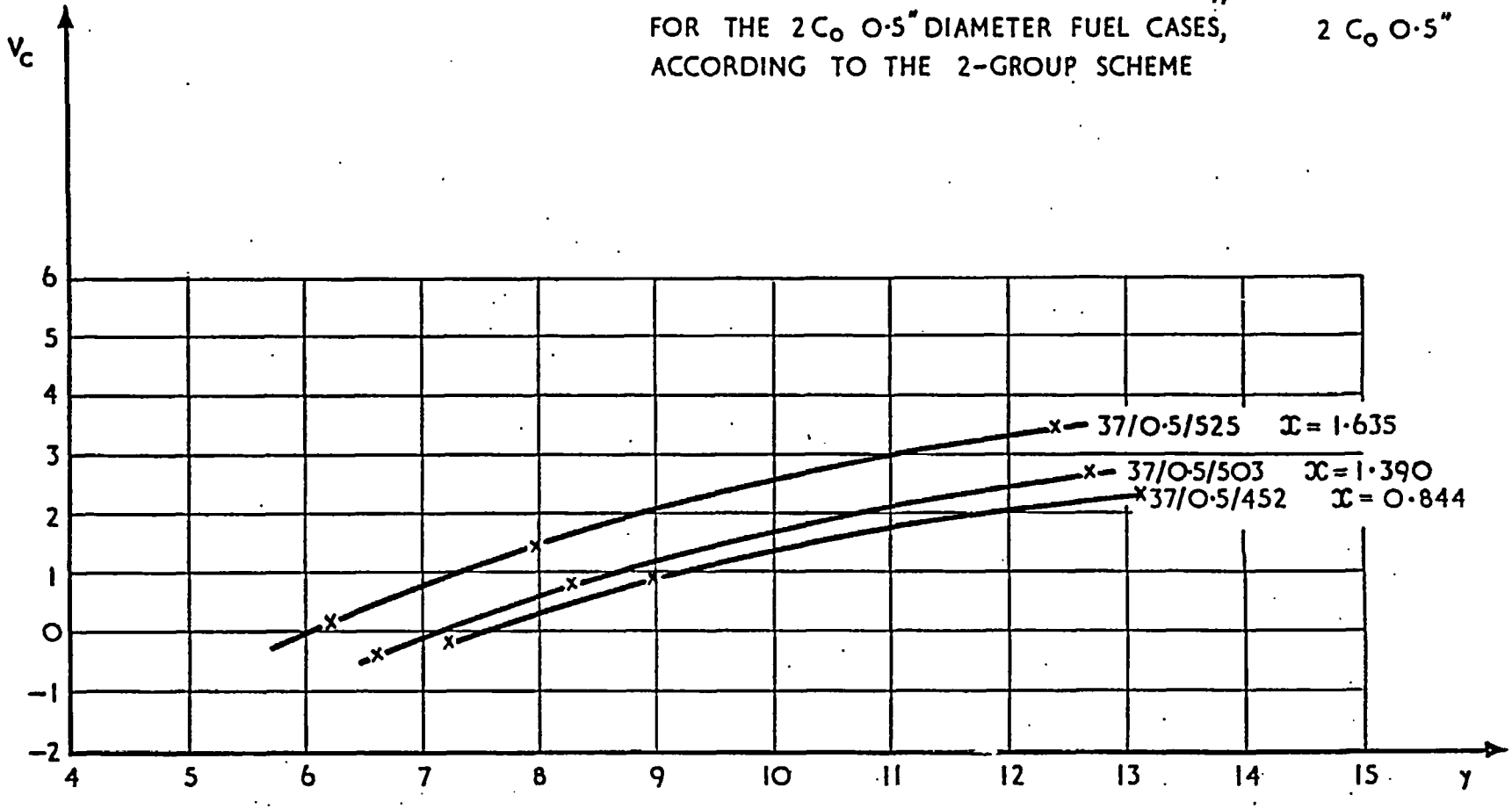
VARIATION OF VOID COEFFICIENT WITH γ,
FOR THE 2 C₀ 0·5" DIAMETER FUEL CASES,
ACCORDING TO THE 2-GROUP SCHEME
2 C₀ 0·5"
V_C
6
5
4
3
2
1
0
−1
−2
4
5
6
7
8
9
10
11
12
13
14
15
γ
37/0·5/525 𝔛 = 1·635
37/0·5/503 𝔛 = 1·390
37/0·5/452 𝔛 = 0·844

FIGURE 21

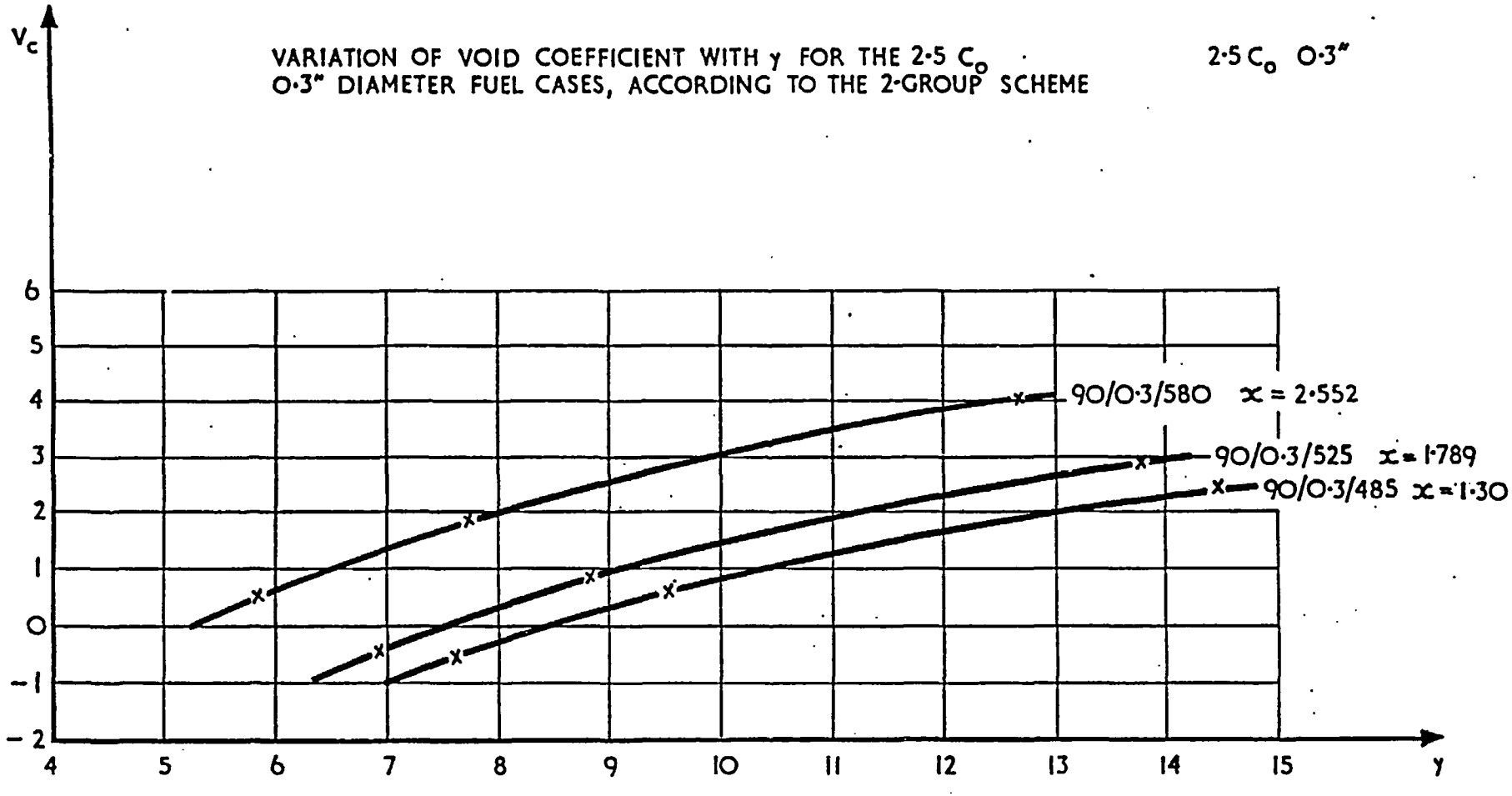
VARIATION OF VOID COEFFICIENT WITH y FOR THE 2·5 C_o 0·3" DIAMETER FUEL CASES, ACCORDING TO THE 2-GROUP SCHEME
2·5 C_o 0·3"
V_c
6
5
4
3
2
1
0
−1
−2
4
5
6
7
8
9
10
11
12
13
14
15
y
90/0·3/580 α = 2·552
90/0·3/525 α = 1·789
90/0·3/485 α = 1·30

FIGURE 22

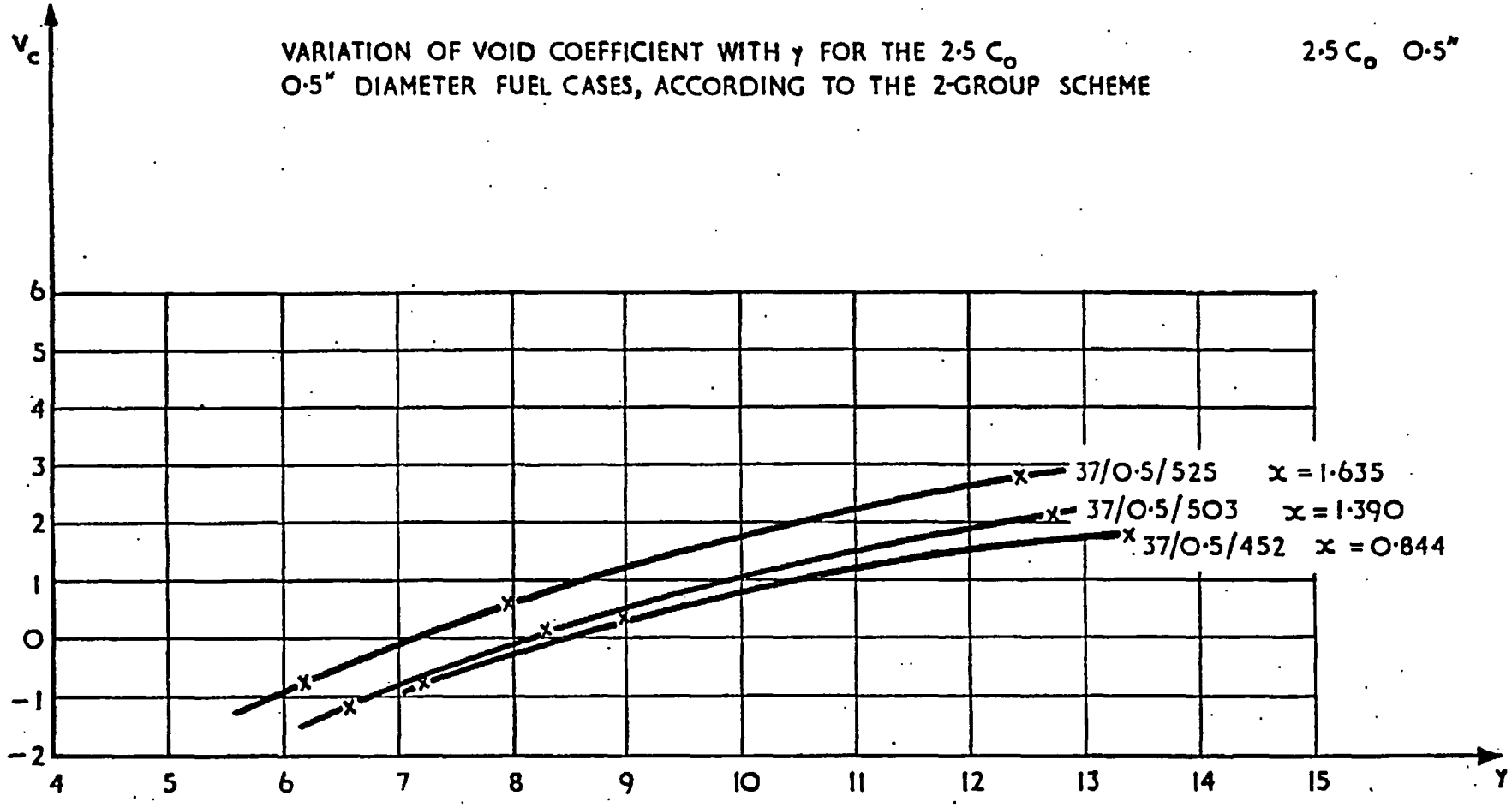
VARIATION OF VOID COEFFICIENT WITH γ FOR THE 2·5 C₀ 0·5" DIAMETER FUEL CASES, ACCORDING TO THE 2-GROUP SCHEME
2·5 C₀ 0·5"
V_c
6
5
4
3
2
1
0
−1
−2
4
5
6
7
8
9
10
11
12
13
14
15
γ
37/0·5/525 x = 1·635
37/0·5/503 x = 1·390
37/0·5/452 x = 0·844

FIGURE 23

CONTOUR MAP OF VOID COEFFICIENT VARIATION WITH x, y FOR THE $1{\cdot}28C_o$, 0·5" CASES.

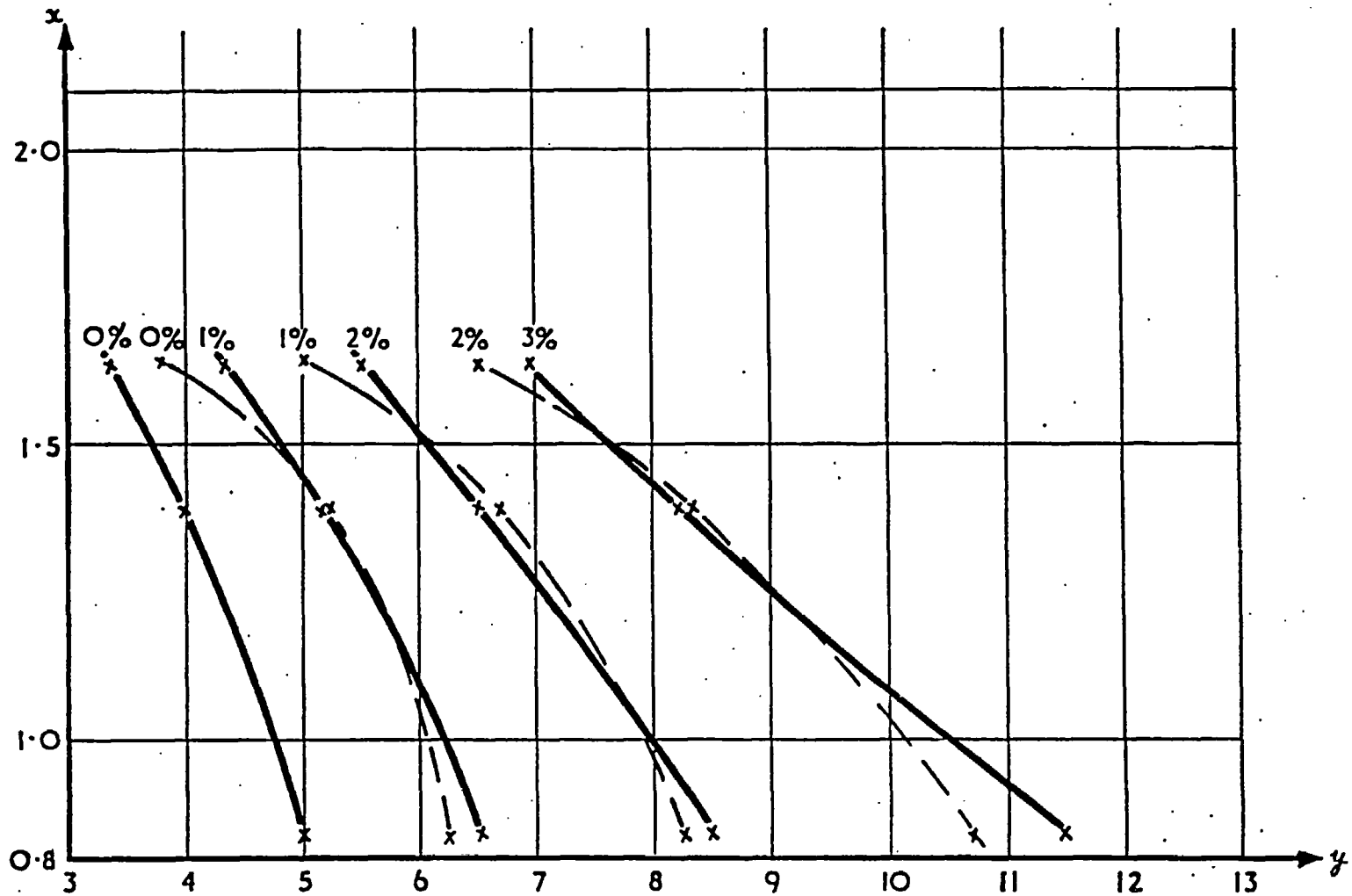

FIGURE 24

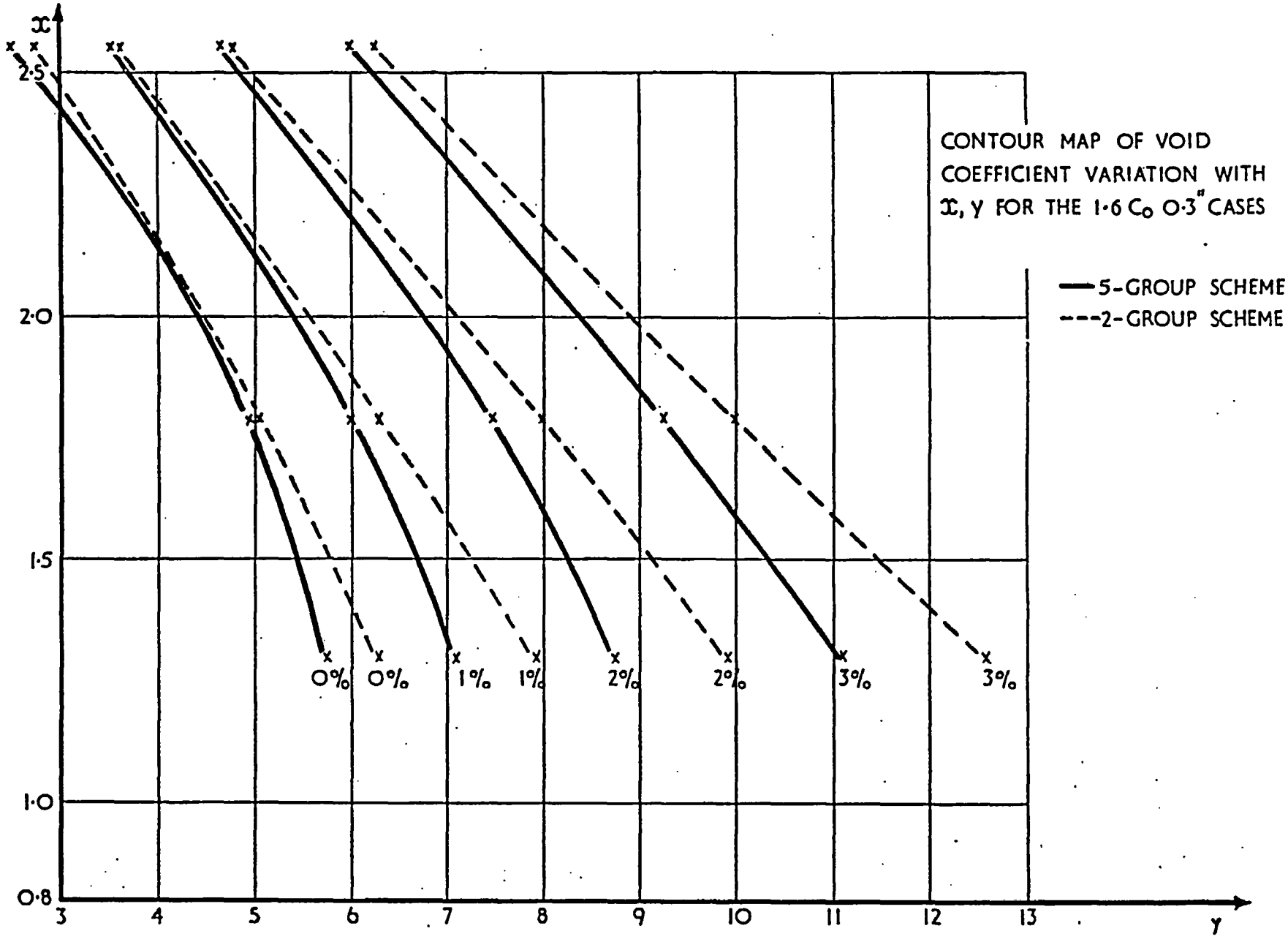
CONTOUR MAP OF VOID COEFFICIENT VARIATION WITH x, y FOR THE 1·6 C₀ 0·3" CASES
5-GROUP SCHEME
2-GROUP SCHEME
x
y
2·5
2·0
1·5
1·0
0·8
3
4
5
6
7
8
9
10
11
12
13
0%
0%
1%
1%
2%
2%
3%
3%

FIGURE 25

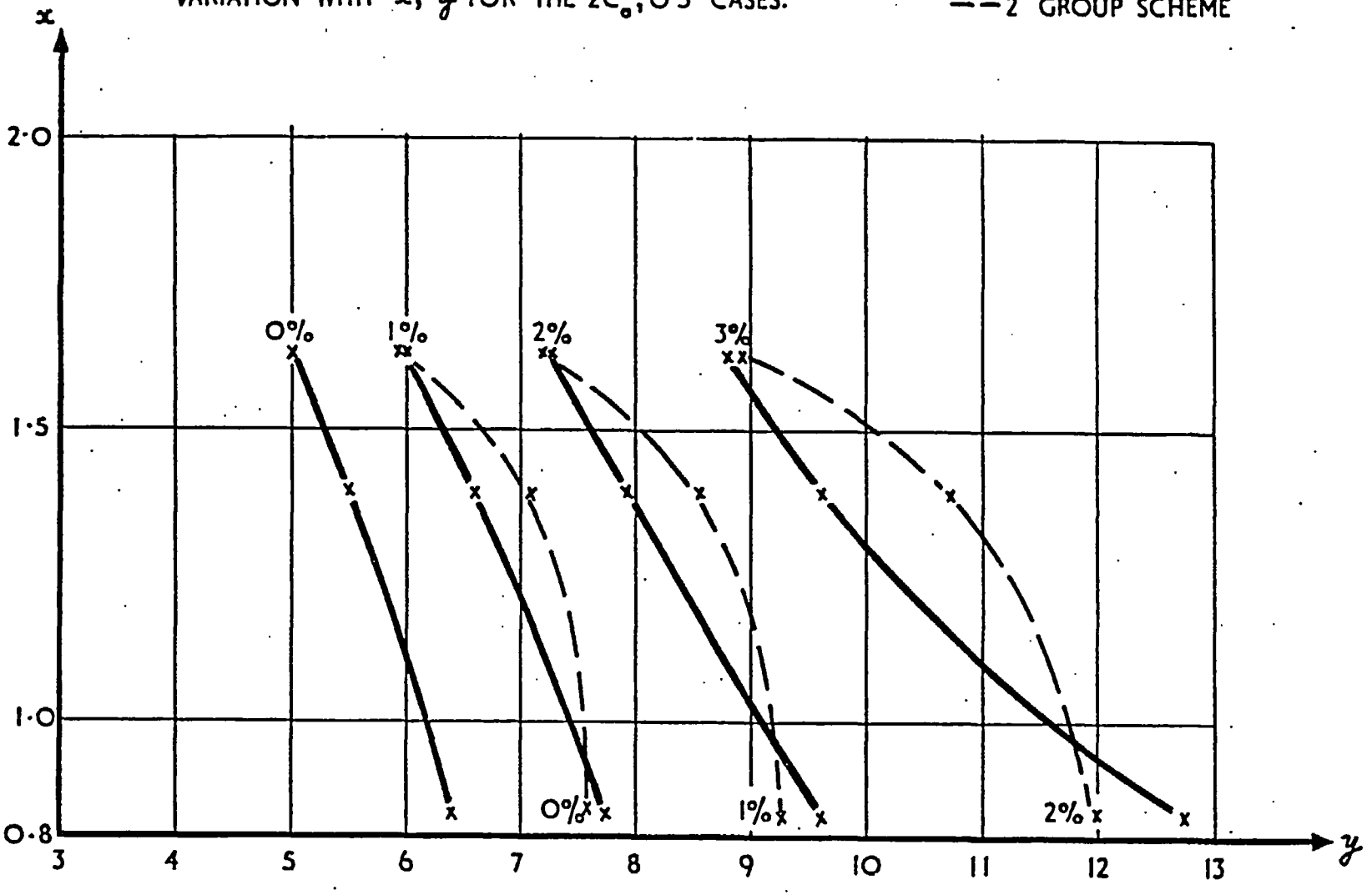
CONTOUR MAP OF VOID COEFFICIENT
VARIATION WITH x, y FOR THE 2C₀, 0·5" CASES.
5 GROUP SCHEME
2 GROUP SCHEME
x
2·0
1·5
1·0
0·8
0%
1%
2%
3%
0%
1%
2%
3
4
5
6
7
8
9
10
11
12
13
y

FIGURE 26

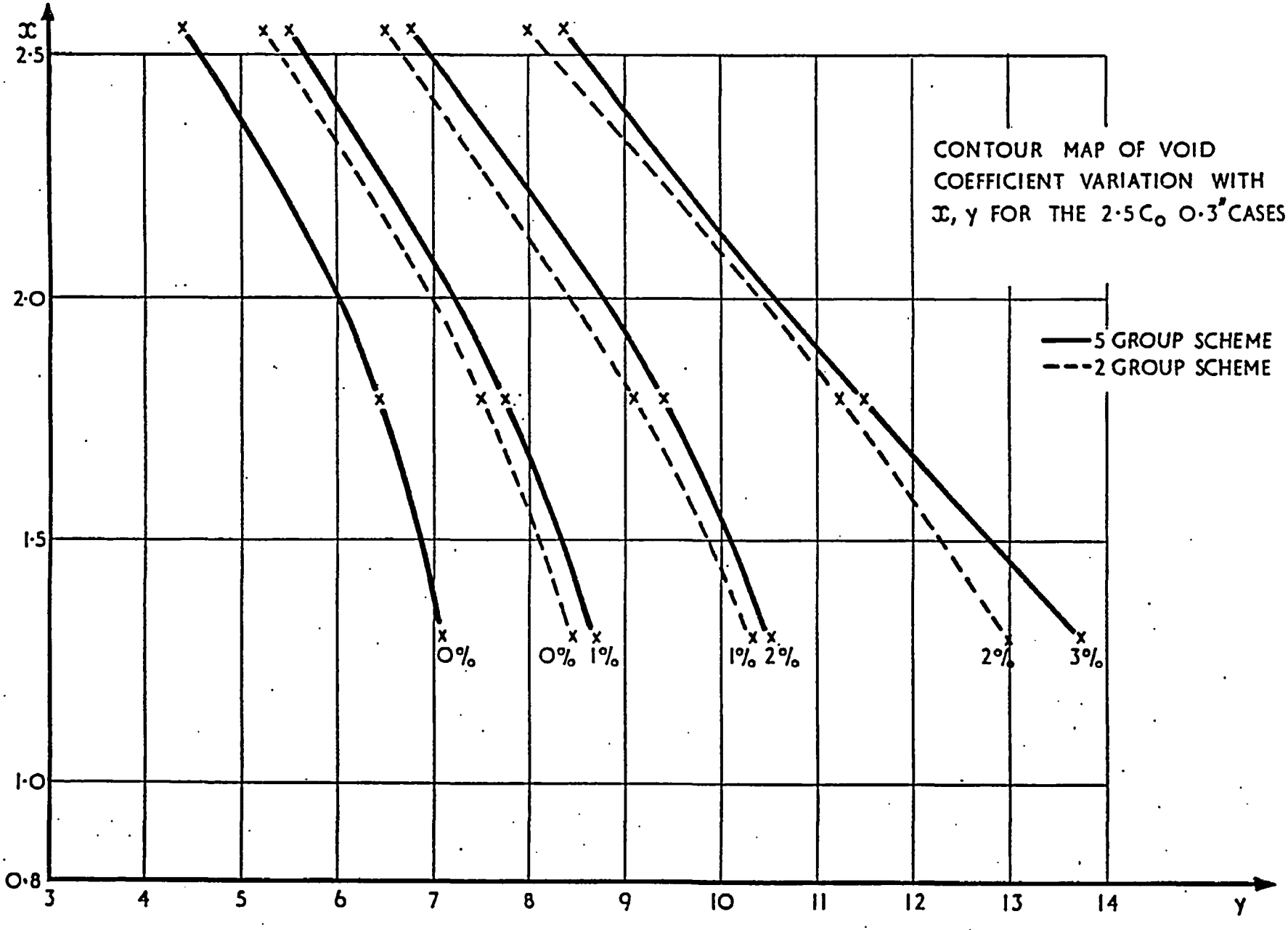
x
2·5
2·0
1·5
1·0
0·8
3
4
5
6
7
8
9
10
11
12
13
14
y
CONTOUR MAP OF VOID COEFFICIENT VARIATION WITH x, y FOR THE 2·5 C₀ 0·3" CASES
5 GROUP SCHEME
2 GROUP SCHEME
0%
0% 1%
1% 2%
2%
3%

FIGURE 27

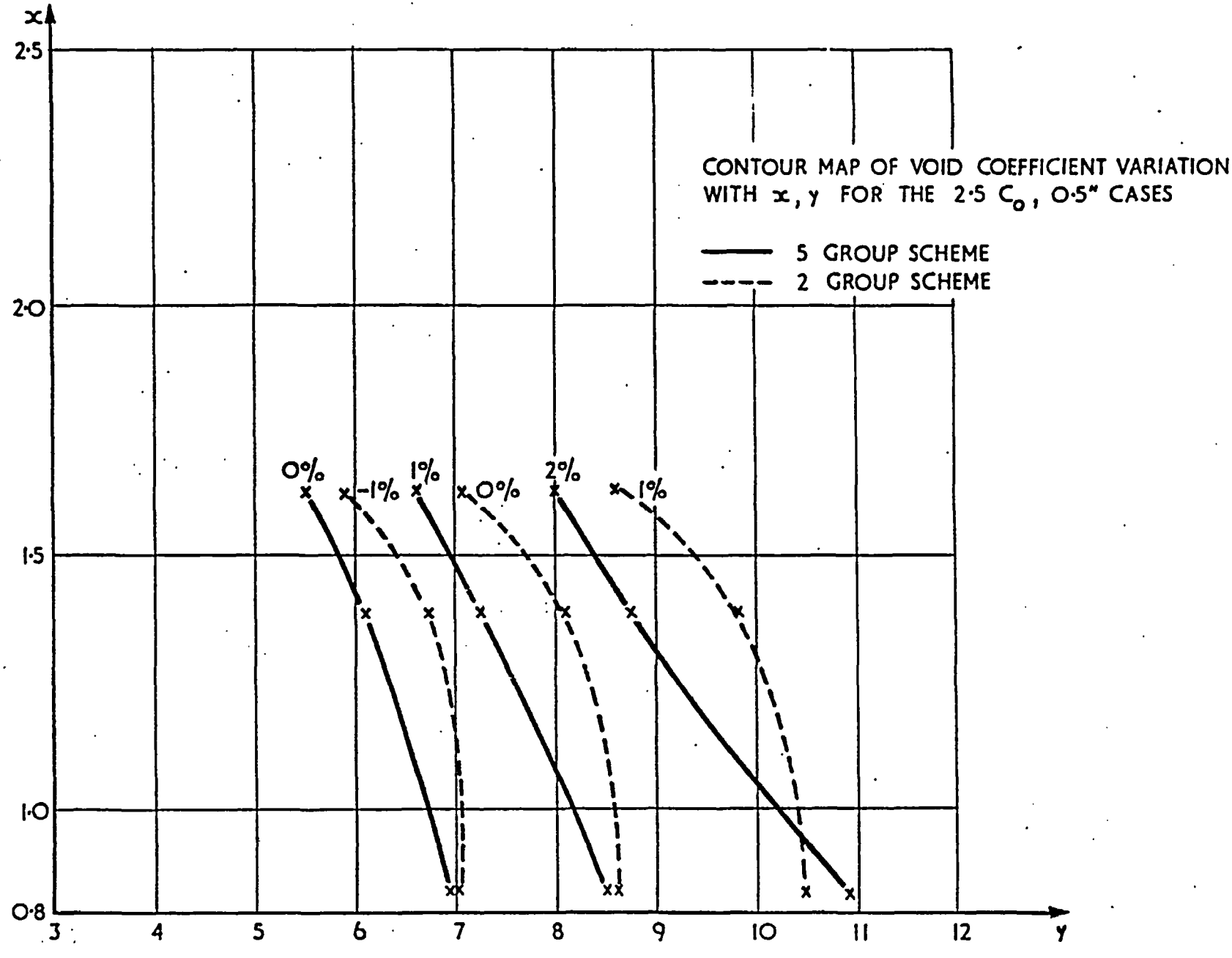
x
2·5
2·0
1·5
1·0
0·8
3
4
5
6
7
8
9
10
11
12
y
CONTOUR MAP OF VOID COEFFICIENT VARIATION
WITH x, y FOR THE 2·5 C_o, 0·5" CASES
5 GROUP SCHEME
2 GROUP SCHEME
0%
-1%
1%
0%
2%
1%

FIGURE 28

DISTRIBUTION

Sir William Cook	Risley

Members of Heavy Water Reactor Steering Committee

Mr. R. V. Moore	Risley
Dr. H. Kronberger	"
Mr. S. Fawcett	"
Mr. F. W. Fenning	"
Mr. C. R. Bennett	"
Mr. P. M. Booocock (4 copies)	"
Mr. N. Bradley	"
Mr. T. J. Heal (P.G.)	"
Mr. C. E. Iliffe	"
Mr. D. S. G. Lewis	"
Mr. V. H. B. Macklen	"
Mr. D. W. Fry (3 copies)	Winfrith
Mr. P. W. Mummery	"
Dr. C. G. Campbell	"
Dr. J. E. R. Holmes	"
Mr. E. C. W. Perryman (2 copies)	Culcheth
Mr. J. Harper (2 copies)	Springfields
Dr. J. K. Dawson	Harwell
Mr. P. H. W. Wolff	English Electric Co.Ltd.
Mr. D. R. Smith	T.N.P.G.
Dr. A. G. H. Coombs	U.P.C.

Members of S.G.H.W./ Specifications Working Party (other than those named above)

Mr. G. K. Dickson	Risley
Mr. A. Green	"
Mr. J. Guild	"
Mr. R. J. Haslam	"
Mr. F. G. Johnson	"
Dr. D. Linning	"
Mr. R. R. Matthews	"
Mr. G. W. Blumfield	Winfrith
Mr. R. J. Cox	"
Mr. W. S. Eastwood	"
Mr. J. Smith	"
Mr. A. E. Williams	Springfields
Mr. P. M. C. Lacey	Harwell

Distribution (contd.)

Additional

Risley

Mr. R. Reynolds
Mr. D. Billington

Culcheth

Mr. J. M. Hutcheon

Springfields

Dr. H. K. Hardy

Windscale

Mr. K. Saddington
Dr. A. J. M. Hitchcock

Harwell

Mr. R. F. Jackson
Dr. P. Murray
Dr. F. A. Vick

Capenhurst

Mr. F. I. Hurley

Winfrith

Dr. F. R. Allen
Dr. J. R. Askew
Mr. A. J. Briggs
Mr. F. G. Chapman
Dr. C. T. Chudley
Mr. D. English
Mr. J. Fell
Dr. W. N. Fox
Mr. T. M. Fry
Mr. A. J. Goddard
Mr. C. P. Gratton
Mr. C. F. Griggs
Dr. D. Hicks
Mr. M. N. John
Mr. I. Johnstone
Mr. G. H. Kinchin
Dr. G. N. Lance
Dr. D. C. Leslie (4 copies)
Dr. R. V. Macbeth
Mr. P. K. M'Pherson
Miss B. Manuell
Mr. D. Moxon
Mr. P.A.B. Murdoch (2 copies)
Mr. D. A. Newmarch
Mr. R. Potter
Mr. I. Pull
Mr. J. Randles
Mr. H. T. Richardson
Mr. M. F. Smith
Dr. R. D. Smith
Mr. R. J. Symes
Mr. W. H. Taylor
Mr. M. J. Terry
Mr. J. G. Tyror
Mr. G. M. Wells
Mr. W. J. Woods
Dr. H. E. Wrigley